Late Maastrichtian and K/T paleoenvironment of the eastern Tethys (Israel): mineralogy, trace and platinum group elements, biostratigraphy and faunal turnovers

Thierry ADATTE[1], Gerta KELLER[2], Doris STÜBEN[3], Markus HARTING[3], Utz KRAMAR[3], Wolfgang STINNESBECK[4], Sigal ABRAMOVICH[5] et Chaim BENJAMINI[5]

Key words. – Cretaceous-Tertiary Boundary, Israel, Iridium, Impact, Volcanism, Paleoclimate and sea-level fluctuations, Biostratigraphy, Chemostratigraphy, Clay mineralogy,

Abstract. – The late Maastrichtian to early Danian at Mishor Rotem, Israel, was examined based on geochemistry, bulk rock and clay mineralogies, biostratigraphy and lithology. This section contains four red clay layers of suspect impact or volcanic origin interbedded in chalk and marly chalks. PGE anomalies indicate that only the K/T boundary red layer has an Ir dominated PGE anomaly indicative of an impact source. The late Maastrichtian red clays have Pd dominated PGE anomalies which coincide with increased trace elements of terrigenous and volcanogenic origins. Deccan or Syrian-Turkey arc volcanism is the likely source of volcanism in these clay layers. Glauconite, goethite and translucent amber spherules are present in the clay layers, but the Si-rich spherules reported by Rosenfeld *et al.* [1989] could not be confirmed. The absence of Cheto smectite indicates that no altered impact glass has been present. The red layers represent condensed sedimentation on topographic highs during sea level highstands. In the Negev area, during the late Maastrichtian, the climate ranged from seasonally wet to more arid conditions during zones CF3 and CF2, with more humid wet conditions in the latest Maastrichtian zone CF1 and in the early Danian, probably linked to greenhouse conditions. Planktic foraminifera experienced relatively high stress conditions during this time as indicated by the low species richness and low abundance of globotruncanids. Times of intensified stress are indicated by the disaster opportunist *Guembelitria* blooms, which can be correlated to central Egypt and also to Indian Ocean localities associated with mantle plume volcanism. Marine plankton thus support the mineralogical and geochemical observations of volcanic influx and reveal the detrimental biotic effects of intense volcanism.

Evolution des paléo-environnements durant le Maastrichtien terminal et la limite Crétacé-Tertiaire dans la Téthys orientale (Negev, Israël) : minéralogie, géochimie, biostratigraphie et renouvellements fauniques

Mots clés. – Crétacé-Tertiaire, Israël, Iridium, Impact, Volcanisme, Fluctuations climatiques et eustatiques, Biostratigraphie, Chimiostratigraphie, Minéralogie, Argiles

Résumé. – A Mishor Rotem, Israël, l'intervalle Maastrichtien terminal-Danien basal a été étudié par le biais d'analyses géochimiques, minéralogiques, biostratigraphiques et lithologiques. Cette section est caractérisée par des craies et des marnes crayeuses au sein desquelles, quatre couches rouges argileuses ont été mises en évidence. L'analyse des éléments du groupe du platine (EGP) a montré que seule la couche rouge correspondant à la limite Crétacé-Tertiaire était dominée par l'Iridium (Ir) et, donc caractéristique d'un impact météoritique. Les trois autres niveaux rouges, situés dans le Maastrichtien terminal (Zone CF1), sont caractérisés par un assemblage de EGP au sein duquel le palladium (Pd) était dominant, indiquant une origine volcanique. Les Trapps du Deccan ou l'arc volcanique syrio-turc pourraient en être la source. De plus, l'abondance d'autres éléments-traces reflète un apport terrigène important. De nombreuses sphérules glauconitiques, de goethite et des gouteletttes d'ambre ont été observées dans les quatre couches, mais la présence de sphérules enrichies en Si (tectites), indiquées par Rosenfeld *et al.* [1989], n'a pu être confirmée. De plus l'absence de smectite bien cristallisée de type Cheto, caractéristique de l'altération des verres d'impacts parle en faveur de l'absence de ces derniers. Ces couches argileuses rouges indiquent une sédimentation réduite sur des paléo-reliefs sous-marins, durant des périodes de haut niveau marin. Le Maastrichtien tardif était caractérisé par des climats à saisons contrastées, tendant à l'aridité (Zone CF3 et CF2), devenant plus humide durant le Maastrichtien terminal (Zone CF1) et le Paléocène basal, ce changement étant probablement lié à l'établissement de conditions à effet de serre. Les assemblages de foraminifères planctoniques sont caractérisés par une faible diversité indicative de conditions de stress assez élevé. Ces périodes de stress coincident avec des blooms du genre *Guembelitria*, un genre oportuniste « désastre », qui peuvent

[1] Geological Institut, University of Neuchatel, CH-2007 Neuchatel, Switzerland. thierry.adatte@unine.ch
[2] Department of Geosciences, Princeton University, Princeton NJ 08544, USA. gkeller@Princeton.edu
[3] Institut of Mineralogy and Geochemistry, University of Karlsruhe, 76128 Karlsruhe, Germany, doris.stueben@bio-geo.uni-karlsruhe.de, utz.kramar@bio-geo.uni-karlsruhe.de
[4] Geological Institut, University of Karlsruhe, P.O. Box 6980, 76128 Karlsruhe, Germany, wolfgang.stinnesbeck@bio-geo.uni-karlsruhe.de
[5] Department of Geological and Environmental Sciences, Ben Gurion University of the Negev, P.O. Box 653, Beer Sheva, 84105 Israel. sigalab@bgumail.bgu.ac.il

être corrélées jusque dans des sections coevalentes localisées en Egypte centrale mais aussi dans l'océan Indien, caractérisées par une activité volcanique liée à un point chaud. De ce fait, l'étude des assemblages de foraminifères planctoniques confirme les observations géochimiques et minéralogiques indiquant un influx volcanique important et met en lumière les effets négatifs d'un volcanisme intense sur la biosphère.

INTRODUCTION

The controversy regarding the cause and nature of the global catastrophe at the Cretaceous/Tertiary (K/T) boundary has reached an impasse with many workers adopting the popular theory that a large impact at Chicxulub on the Yucatan Peninsula in Mexico caused a sudden mass extinction of organisms ranging from planktic foraminifera to dinosaurs [e.g. Alvarez *et al.*, l980; Smit, l990, 1999; Olsson, l997; Molina *et al.*, l998; Bralower *et al.*, 1998; Fastovsky, l996]. But others maintain that the mass extinction was more gradual beginning with high-stress conditions well before the K/T boundary and exacerbated by ongoing environmental changes, including volcanism, climate and sea level variations, with an impact as final contributing factor [e.g. Keller, l988, 2001; Johnson and Kauffman, l996; Courtillot *et al.*, l996].

As a result, new attention has focused on paleoclimatic and paleoceanographic changes during the late Maastrichtian. In particular, the last half million years of the Maastrichtian has become increasingly recognized as a time of rapid and extreme climate changes characterized by 3-4°C greenhouse warming between 65.4 and 65.2 Ma [Barrera, l994; Li and Keller, 1998a], coeval faunal turnover [Abramovich *et al.*, l998; Kucera and Malmgren, l998; Li and Keller, l998b; Olsson *et al.*, 2001], and major Deccan volcanic activity [Courtillot *et al.*, 1996; Hoffmann *et al.*, 2000]. Until recently, a major pulse in Deccan volcanism and CO_2 release seemed the only likely cause for the greenhouse warming. But the recent discovery of three to four glass spherule layers in numerous late Maastrichtian sections from northeastern Mexico with the stratigraphically oldest spherule layer near the base of the *Plummerita hantkeninoides* zone at about 65.3 Ma [Stinnesbeck *et al.*, 2001], suggests that multiple impacts (e.g. comet shower) may also have played a critical role in destabilizing the environment [Keller, 2001; Keller *et al.*, 2002, 2003a]. Recently, Ellwood *et al.*, [2003] noted evidence for a possible pre-K/T boundary impact in the Abat Ouest section, Oman. Apart from the typical Ir anomaly characterizing the K/T boundary, they observed 1.34 m below the K/T a second Ir anomaly coinciding with increased Ni, Cr, As and Zn contents, small iron spherules, but no significant decrease in $\delta^{13}C$ stable isotopes. This level may represent a pre-K/T boundary impact.

If multiple impacts occurred near the end of the Cretaceous, evidence ought to be found in regions outside Mexico. Though a systematic search for impact evidence before or after the K/T boundary has yet to be conducted, such evidence may have been found by Rosenfeld *et al.* [l989, p. 474] who reported "microspherules of different colors and chemical compositions in three late Maastrichtian layers" from the Mishor Rotem section at Makhtesh Gadol in the Negev, Israel (fig. 1). We examined this section in an effort to determine the age and geochemical similarity of the reported spherule deposits and compare them with those in Mexico. Although we were unable to confirm the presence of glass spherules, the results of our high-resolution multidisciplinary study provides critical information on the nature of late Maastrichtian paleoenvironmental changes in the eastern Tethys region and their probable relationship to environmental changes in northeastern Mexico. Here we report the results of detailed stratigraphic, faunal, mineralogical and geochemical (PGE and trace element) analyses of the Mishor Rotem section that span approximately the last 1 m.y. of the Maastrichtian. This report focuses on the evaluation of (1) the sedimentary record based on field observations and mineralogy to determine the nature of deposition, sea level and climate changes, (2) the age, biostratigraphy and completeness of the record, (3) faunal turnovers with respect to ongoing paleoenvironmental changes, (4) trace elements and platinum group elements (including Ir) and their origin, whether terrestrial or cosmogenic, and (5) the nature and origin of the spherules.

LOCATION AND PALEOGEOGRAPHICAL SETTING

The Mishor Rotem section is located approximately 10 km north of the Oron phosphate mine on the road towards Dimona (Israel coordinates 1548/0416). The outcrop is part of the Rotem syncline east of the Hatira anticline (fig. 1). This syncline is part of the Syrian arc structural province of northeast trending gentle folds, which began in the Santonian and continued into the Tertiary. At the time of late Maastrichtian sediment deposition the anticlines and synclines were completely submerged at outer neritic to upper bathyal depths. In southern Israel, alternating units of marls, marly limestones and chalks that form the Ghareb Formation were deposited in an open marine environment at outer neritic to bathyal depths (300-500 m) as indicated by benthic foraminifera (e.g. *Cibicidoides succeedens, C. pseudoacutus, C. hyphalus, Alabamina midwayensis, Angulogavellinella avnimelechi*) [see also Luger, l988; Speijer, l994]. At Mishor Rotem, the section is characterized by three distinct red layers, which are interbedded in late Maastrichtian chalks and marls (fig. 2). Additional outcrops containing these red layers can be traced laterally along the hillside, as well as to the south and west in the areas of Givat Mador and Ein Mor.

Sediments are rich in planktic and benthic foraminifera, ostracods, fish debris and occasional brachiopods. In the region of the Rotem syncline (Makhtesh Gadol) the Maastrichtian Ghareb Formation reaches a thickness of 60-80 m and consists of chalks, marly limestones and marls. The overlying Taqiye Formation is of Paleocene age and consists predominantly of marls that reach a thickness of about 40-50 m. Paleogeographic reconstructions show that this section was located some 5,000-6,000 km from the Deccan magmatic province and was paleoceanographically mainly

influenced by westward flowing surface circumglobal Tethys currents [Camoin *et al.*, 1993].

METHODS

In the field the section was trenched to obtain fresh unweathered surfaces, the sediments measured and examined with respect to lithological changes, bioturbation, macrofossils, sedimentary structures, and erosional surfaces or undulating contacts. Samples were collected at 10 cm intervals and at closer sample intervals across the red layers and K/T boundary. The thin fissile red clay layers at the base of the red marls and at the K/T boundary were sliced out for geochemical analysis and acid concentration to search for

spherules. Samples were processed for foraminiferal analysis following the standard method of Keller *et al.* [l995]. Age and biostratigraphic control is based on quantitative planktic foraminiferal analysis of sample splits of about 300 specimens of the > 63 µm and > 150 µm size fractions that allows evaluation of both small and large species populations. Foraminifera are relatively well preserved morphologically, but test shells are completely recrystallized and infilled with blocky calcite and in some layers silica. Internal molds of foraminifer tests and isolated spherical chamber infillings of silica are common in acid residues. The section is thus not suitable for stable isotope analyses.

Whole rock and clay mineral analyses were conducted at the Geological Institute of the University of Neuchatel,
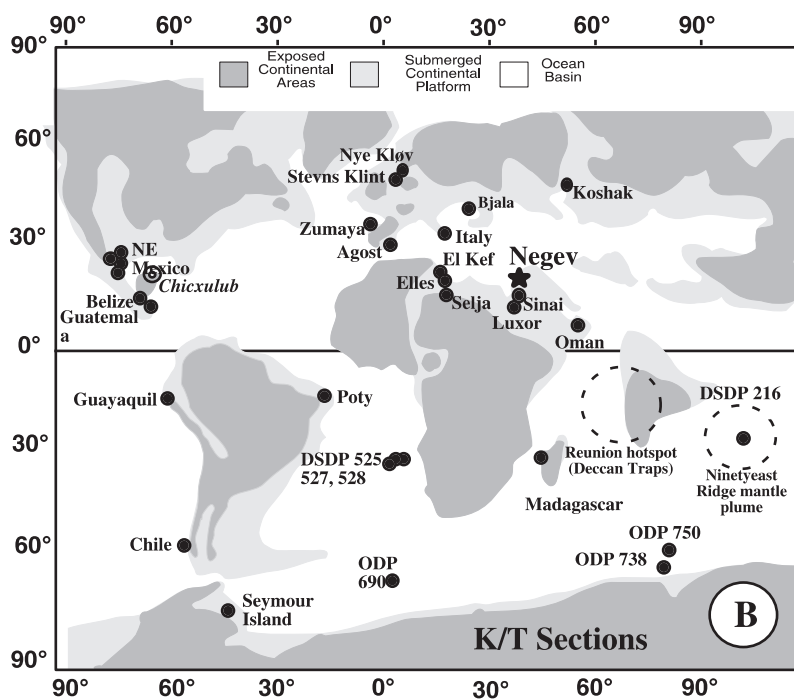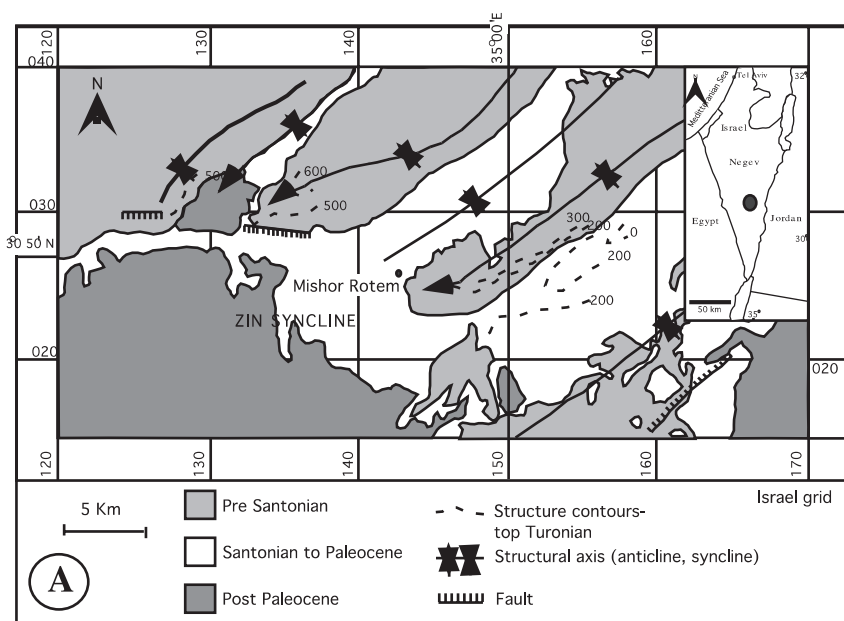

FIG. 1. - A) Location map of Israel and Egypt showing geography of the Mishor Rotem section. B) Paleolocations of Cretaceous-Tertiary (K-T) boundary sections which have good biostratigraphic control and relatively continuous sediment records [modified from Macleod and Keller, 1991]

FIG. 1. - A) *Carte de localisation de la section de Mishor Rotem.* B) *Carte paléogéographique indiquant la localisation des coupes Crétacé-Tertiaire (C-T) montrant un bon contrôle biostratigraphique et un enregistrement sédimentaire continu.*
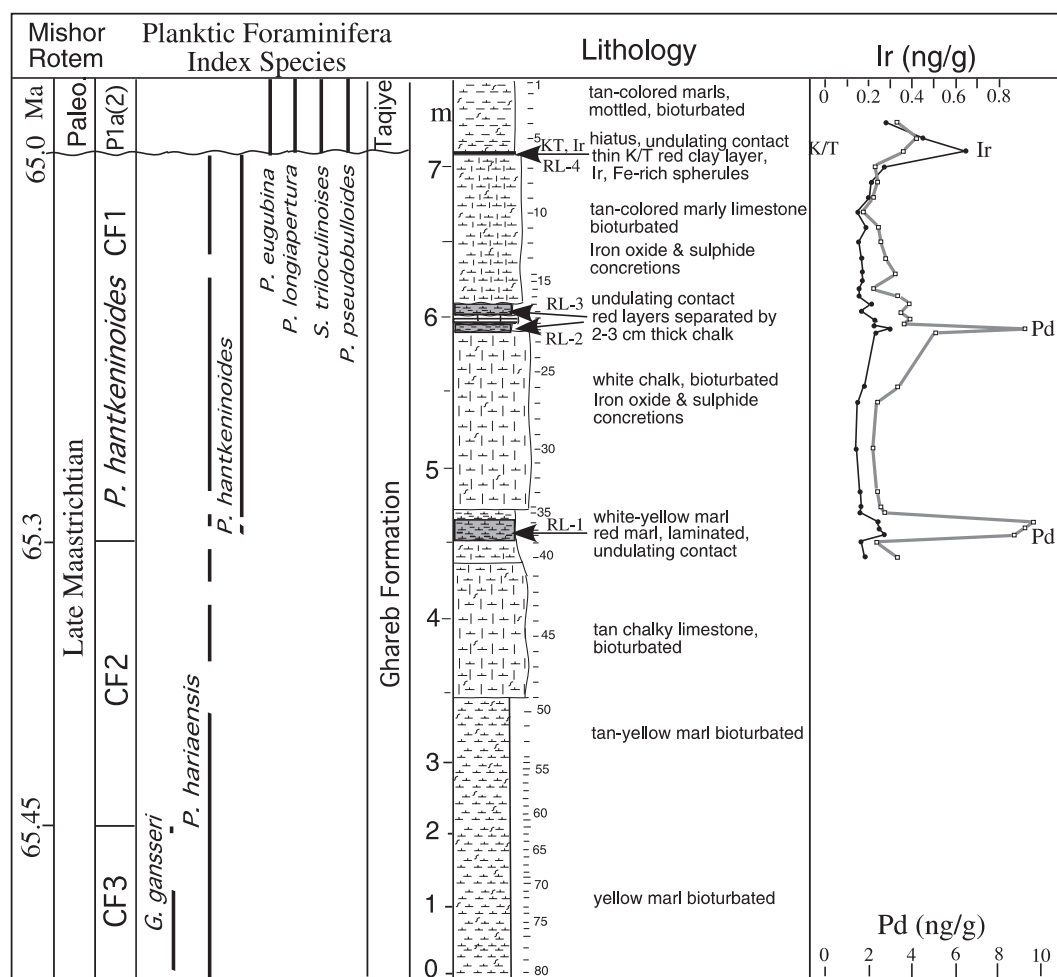
Bull. Soc. géol. Fr., 2005, nº 1

F<small>IG</small>.2. - Lithologic description, biostratigraphy, Ir and Pd anomalies of the Mishor Rotem section. Note the Ir anomaly at the K/T boundary is associated with a red clay layer which infills depressions of an undulating erosion surface. Red marl layers 1 and 2 (RL-1, RL-2) contain Pd anomalies, but only minor Ir enrichments.

F<small>IG</small>. 2. - *Description lithologique, biostratigraphie et localisation des anomalies en Ir et Pd dans la coupe de Mishor Rotem. L'anomalie en Ir de la limite K/T est localisée dans une couche argileuse rouge remplissant les dépressions liées à une limite érosive ondulée. Les couches marneuses 1 et 2 (RL-1 et RL 2) contiennent des anomalies en Pd, mais ne sont que faiblement enrichies en Ir.*

Switzerland, based on XRD analyses (SCINTAG XRD 2000 Diffractometer). Sample processing followed the procedure outlined by Kübler [1987] and Adatte *et al.* [1996]. Bulk rock contents are obtained using standard semiquantitative techniques based on external standardisation [Kübler, l983, l987].

Platinum group elements (PGE) were analyzed by ICP-MS after preconcentration and matrix reduction by Ni-fire assay [Kramar *et al.*, 2001; Stueben *et al.*, 2002]. Before the fire assay, samples were spiked with 500 µl of a solution containing about 16 ng of Ir, 10 ng Ru, 33 ng Pd and 33 ng Pt strongly enriched in the isotopes Ir^{191}, Ru^{99} Pd^{105} and Pt^{198}, respectively. The analysis was carried out by isotope dilution mass spectrometry with a ICP/MS (PQ2 from VG Elemental, UK).

Major and trace element distribution was carried out by wave and energy dispersive XRF (Spectrace 5000, Siemens SRS 303 HS) based on methods described in Kramar ([997] and Kramar *et al.* [2001] A total of 30 samples were selected spanning the late Maastrichtian red layers and the K/T boundary.

LITHOLOGY

The late Maastrichtian exposure of the Ghareb Formation at the Mishor Rotem section consists of about 9 m of horizontally stratified white, tan or yellow bioturbated chalks and marly limestones that form resistant beds, separated by three thin layers of laminated red marls stained by iron oxides and hydroxides. For this study, the topmost 7 m of the Ghareb Formation and basal 50 cm of the Taqiye Formation were sampled (fig. 2).

The lower 3.5 m of the section consist of bioturbated yellow marls, which change to tan-yellow marls in the upper 0.5 m interval. Overlying this unit is a 1 m thick resistant, bioturbated, tan-colored chalky limestone. An undulating surface marks the contact between the chalk and overlying 10 cm thick laminated red marl that marks the first red layer (RL-1) that was reported as enriched in glass spherules by Rosenfeld *et al.* [1989]. This RL-1 is a dark rusty red colar and fissile at the base, but grades upwards into bioturbated yellow-white marls with flaser-bedding. Overlying this unit is a 1.2 m thick resistant white

bioturbated, chalky limestone rich in iron oxide and sulphide concretions. This unit grades into the second 10 cm thick flaser-bedded and bioturbated red marl layer (RL-2) from which spherules were reported. A 2-3 cm thick red stained chalk layer separates this red marl from the third 10 cm thick red marl layer (RL-3) with reported spherules (fig. 2). Undulating surfaces mark the base and top of the overlying 2 m thick tan-colored marly limestones with iron oxide and sulphide concretions. The top of this unit represents the top of the Maastrichtian and the Ghareb Formation. The three red layers are thus within zone CF1 that spans the last 300 kyr of the Maastrichtian, though the undulating surfaces suggest that part of this interval is missing due to erosion. This is reflected by the unusually low average sedimentation rate of 0.83 cm/1000 yrs for zone CF1 and 1.6 cm/1000 yrs for CF2 (fig. 2).

The K/T boundary is between the lithological break flanked by tan marly limestone of the Ghareb Formation and tan marls of the Taqiye Formation. The dark boundary clay layer that characterizes the K/T boundary in the most complete sections is not present at Mishor Rotem, nor has it been reported from other sections in Israel due to a K/T unconformity [Rosenfeld *et al.*, l989; Keller and Benjamini, l991; Abramovich *et al.*, l998; Speijer, 1994]. At Mishor Rotem a hiatus also marks the K/T transition as observed by the undulating erosional contact at the top of Maastrichtian tan limestone. However, the characteristic thin K/T red layer (2-4 mm, labeled RL-4) is discontinuously present in depressions of the undulating erosional surface.

BIOSTRATIGRAPHY

The Mishor Rotem section of the Makhtesh Gadol area of the Negev is the first locality in Israel where a thin K/T boundary clay layer with iron spherules and Ir anomaly has been found [Rosenfeld *et al.,* l989]. In other published localities throughout southern Israel, the K/T boundary clay and most of the early Danian is missing due to erosion

[Magaritz *et al.,* l985; Rosenfeld *et al.,* l989; Keller and Benjamini, l991]. To evaluate the nature and continuity of the sedimentary record, the biostratigraphy is evaluated based on the Cretaceous foraminiferal (CF) zonal scheme by Li and Keller [l998a,b], which replaces the *Abathomphalus mayaroensis* zone with four zones and provides much improved age control for the late Maastrichtian. The upper three of these four zones are recognized in the Mishor Rotem section as shown in figures 2 and 3.

The late Maastrichtian at the base of the section is characterized by zone CF3, which defines the interval from the first appearance of *Pseudoguembelina hariaensis* to the last appearance of *G. gansseri* (66.83-65.45 Ma, figs 3, 4). The presence of these two index species in the lower 2 m of the section analyzed at Mishor Rotem indicate that at least the upper part of zone CF3 is present (fig. 2). Zone CF2, which marks the interval from the last appearance of *Gansserina gansseri* to the first appearance of *Plummerita hantkeninoides* (fig. 3), spans from 2 m to 4.5 m and just below the first red layer (RL-1). The average sediment accumulation rate within this zone is 1.6 cm/1000 yrs, and suggests very low sedimentation, or a short hiatus. The uppermost 4.5 m of the Ghareb Formation below the K/T boundary mark the range of *Plummerita hantkeninoides*, which spans the last 300,000 kyr of the Maastrichtian and defines zone CF1 [Pardo *et al.,* l996; Li and Keller, 1998a,b]. The average sediment accumulation rate within this zone is only 0.83 cm/1000 yrs and indicates short hiatuses at undulating surfaces (e.g. below the K/T boundary and red layers) and condensed sedimentation (red layers). The K/T boundary is marked by an undulating erosional surface that marks the top of the last resistant chalk layer and underlies the K/T boundary (fig. 2).

Lithologically, a complete K/T transition is characterized by a boundary clay layer (which marks zone P0) with a thin red layer at the base, which generally contains the Ir anomaly. Biostratigraphically, zone P0 is defined as the interval between the extinction of Cretaceous tropical and subtropical planktic foraminifera and the first appearance of *Parvularugoglobigerina eugubina* and/or *P. longiapertura*

FIG. 3. - Planktic foraminiferal biozonation of the Mishor Rotem section based on the zonal scheme by Li and Keller [l998a,b]. Age estimates for late Maastrichtian biozones are based on foraminiferal datum events of DSDP Site 525 and Agost, Spain, tied to the paleomagnetic stratigraphy of the same sections. Note there is a short hiatus at the K/T boundary with the lower part of the *P. eugubina* zone (subzone Pla(l)) removed. The boundary red clay layer and Ir anomaly are present in depressions of an undulating erosional surface that marks the top of the Ghareb Formation.

FIG. 3. - *Biozonation de la coupe de Mishor Rotem, basée sur les foraminifères planctoniques [zonation de Li et Keller, 1998a,b]. Les âges des biozones du Maastrichtien supérieur sont basés sur les données du forage DSDP 525 et la coupe d'Agost, corrélées avec les données paléomagnétiques. Il faut souligner le court hiatus coincidant avec la limite K/T et qui comprend la partie inférieure de la zone à P. Eugubina. L'anomalie en Ir observée dans la couche argileuse rouge de la limite K/T est localisée dans les dépressions d'une surface d'érosion qui marque le sommet de la formation Ghareb.*
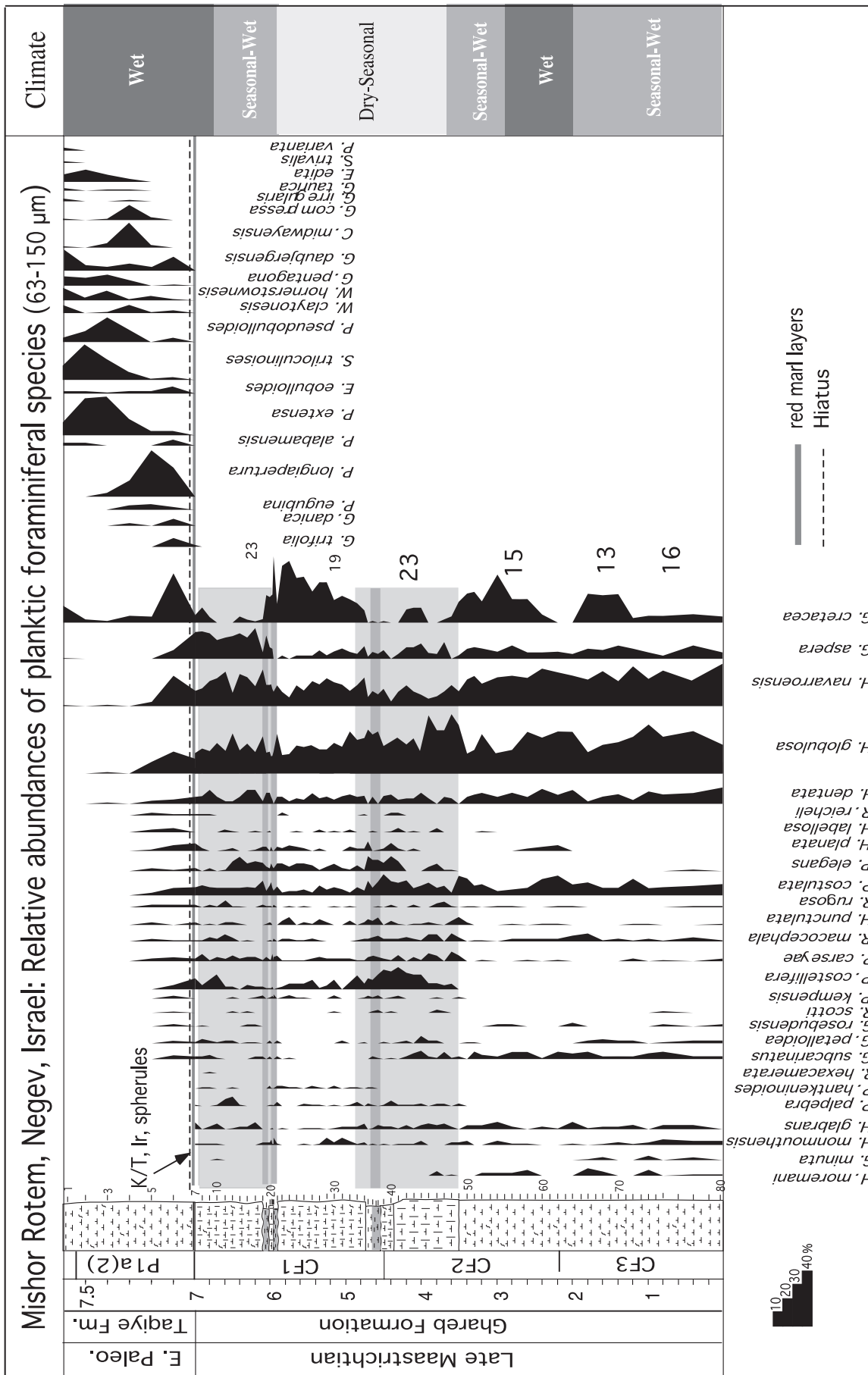
42   ADATTE T. *et al.*

FIG. 4. – Relative abundance of planktic foraminifera in the 63-150 µm size fraction and inferred climate based on clay mineralogy at Mishor Rotem, Israel. Note the low species diversity, dominance of low oxygen tolerant heterohelicids (*H. globulosa, H. navarroensis*), and blooms of the opportunist *Guembelitria* in the late Maastrichtian. Presence of common Cretaceous species in early Danian sediments is due to reworking. Shaded intervals mark increased species diversity and absence of opportunists. Gray lines mark red marl layers, dashed line at K/T boundary marks hiatus.

FIG. 4. – *Abondances relatives des foraminifères planctoniques de la fraction 63-150 µm dans la coupe de Mishor Rotem et fluctuations climatiques déduites des minéraux argileux. Il faut souligner la faible diversité spécifique, la dominance des hétérohélicidés tolérant des milieux peu oxygénés (H. globulosa, H. navarroensis) et les blooms du genre opportuniste Guembelitria durant le Maastrichtien tardif. La présence d'espèces crétacées dans les sédiments du Danien précoce est due à des remaniements. Les intervalles ombrés indiquent une augmentation de la diversité spécifique et l'absence des espèces opportunistes. Les lignes grises indiquent les couches marno-argileuses rouges, le trait pointillé indique un hiatus à la limite K/T.*

(fig. 4) [Keller *et al.,* l995]. At Mishor Rotem, zone P0 is partially present in the form of the thin red layer and Ir anomaly of 0.65 pbb [as also reported by Rosenfeld *et al.,* l989], which infill depressions of the undulating surface of the Maastrichtian chalk. The first Danian species appear in the marls immediately above the red layer along with many Cretaceous species that reflect reworking, as also observed in many other section in southern Israel [Keller and Benjamini, l991].

The early Danian shaly marl of the Taqiye Formation at Mishor Rotem contains a diverse early Danian assemblage, including the index species *Parvularugoglobigerina eugubina, Parasubbotina pseudobulloides* and *Subbotina triloculinoides,* which mark the upper part of zone Pla, here labeled subzone Pla(2) (fig. 2). Since this subzone directly overlies the boundary red layer, a short hiatus is present and spans the lower part of the *P. eugubina* zone (subzone Pla(1)). A hiatus is also suggested by the presence of early Danian species in the 63-105 µm size fraction, which generally do not occur until subzone Pla(2), and by the abundance of reworked Cretaceous species near the base of subzone Pla(2). An early Danian Pla(l)/Pla(2) hiatus has been observed in all other studied sections of the Negev [Keller and Benjamini, l991], and in many early Danian sections worldwide [MacLeod and Keller, l991].

FAUNAL TURNOVER

Planktic foraminiferal assemblages from the Mishor Rotem section are of unusually low diversity for the eastern Tethys, averaging 30 species as compared with 40-50 species at El Kef, Tunisia [Li and Keller, l998b]. Species populations which are consistently present are shown in figure 4 based on analysis of the 63 microns size fraction. The late Maastrichtian assemblages are dominated by small biserial heterohelicids (*Heterohelix globulosa, H. dentata, H. navarroensis)*, small trochospiral forms (*Globigerinelloides aspera, Rugoglobigerina rugosa, Hedbergella monmouthensis*), intermittent peak populations of *Guembelitria cretacea*, and in zone CF1 *Pseudoguembelina costellifera, P. costulata, P. carseyae, Pseudotextularia elegans)*. Globotruncanids and other tropical species (e.g. *Racemiguembelina, Planoglobulina*) are very rare or absent. In the first 20 cm above the K/T boundary, reworked Maastrichtian species are abundant, along with common to abundant species indicative of early Danian subzone Pla(2) (e.g. *Parvularugoglobigerina eugubina*, *P. longiapertura*, *Globoconusa daubjergensis*, *Parasubbotina pseudobulloides*, *Subbotina triloculinoides*, fig. 4). The unusual abundance of reworked Cretaceous species reflects current activity and a hiatus (most of zone P0 and Pla(l) missing).

Faunal assemblages show a strong correlation with marl and chalk lithologies. In the 3.5 m thick marls at the base of the section there is a greater dominance of low oxygen tolerant heterhelicids (*H. globulosa*), lower species diversity (13-16 as compared with 19-23 species, fig. 4) and absence of tropical species, which indicates relatively cool waters and a well defined oxygen minimum zone. Variable high stress conditions are indicated by two intervals of peak abundance of *Guembelitria cretacea* (30-40%,), an ecological opportunist that thrived in surface waters at times of

high stress. In contrast, the marly chalks above this interval reflect significantly warmer climatic conditions and a well stratified watermass (shaded intervals, fig. 4), as indicated by higher species diversity (23 species consistently present) and increased presence of tropical species (e.g. *Pseudotextularia, Pseudoguembelina*) and ecological generalists (e.g. *Rugoglobigerina, Hedbergella, Globigerinelloides*). However, peak *Guembelitria* abundance (50%) between the red layers (lower part of CF1) suggests increased biotic stress, as also suggested by reduced diversity from 23 to 19 species. The red marl layers do not correlate with any unusual faunal patterns and reveal no increased biotic stress for planktic foraminifera.

SPHERULES IN RED LAYERS

Our interest in the Mishor Rotem section stems from the Rosenfeld *et al.* [l989] report of abundant (~ 1000 spherules per 100 g sediment) silica-rich microspherules of 100-150 µm in diameter in the three red layers. They described translucent yellow spherules with K-Al-feldspar compositions, dull brown and green spherules composed of Mg-Fe-Al silicates with high FeO concentrations (17-20%), and black spherules with 50% Fe_2O_3, 29% SiO_2 and 12% NiO.

We processed samples from the red layers by acid concentration. The residues consist mainly of foraminiferal chamber infillings by silica or iron, with the spherical chambers that constitute the foraminiferal tests often broken apart and forming great quantities of isolated dull yellow silica spherules, or fewer brown-red iron spherules. Most of the spherules bear small markings of the original attachment in the foraminiferal test. These are possibly some of the microspherules described by Rosenfeld *et al.* [l989, Table 2, p. 479] as "yellow" with high SiO_2 (65%), Al_2O_3 (15%) and, K_2O (15%) values.

Also very abundant in acid residues are the dull green and brown spherules reported by Rosenfeld *et al.* [l989], although much of this material is not really spherical. These are glauconite spherules. The chemical composition listed by these authors is within the range of characteristic glauconites [Odin, 1988]. There are also a number of dull black to brown Fe-rich spherules of probable manganese and iron hydroxides composition, which may correspond to the black spherules listed in Rosenfeld *et al.* [1989].

We also found light yellow and darker amber colored translucent spherules in the 300-400 µm size range that are restricted to the basal 0.5 cm of red layers RL-1 to RL-3. These spherules are glassy in appearance with smooth surfaces, concoidal fractures, and frequently zoned outer rims (fig. 5). Some spherules have residual calcite crystals on the outer surface or on broken fragments, others have tiny air bubble inclusions. The light yellow spherules have chemical composition, which are almost pure carbon (~ 90-95%), though some show sulfur concentrated in zoned outer rims, whereas the darker yellow to amber colored spherules contain significant sulfur throughout the carbon spherules.

Various tests were performed to deduce the nature and origin of these spherules. They do not dissolve in hydrofluoric acid and therefore are not glass, but they burn at 350°C. This suggests that these are amber spherules, possibly from nearby land areas (conifer forests?). The relatively common presence (1 spherule per 100 g of sediments) of these
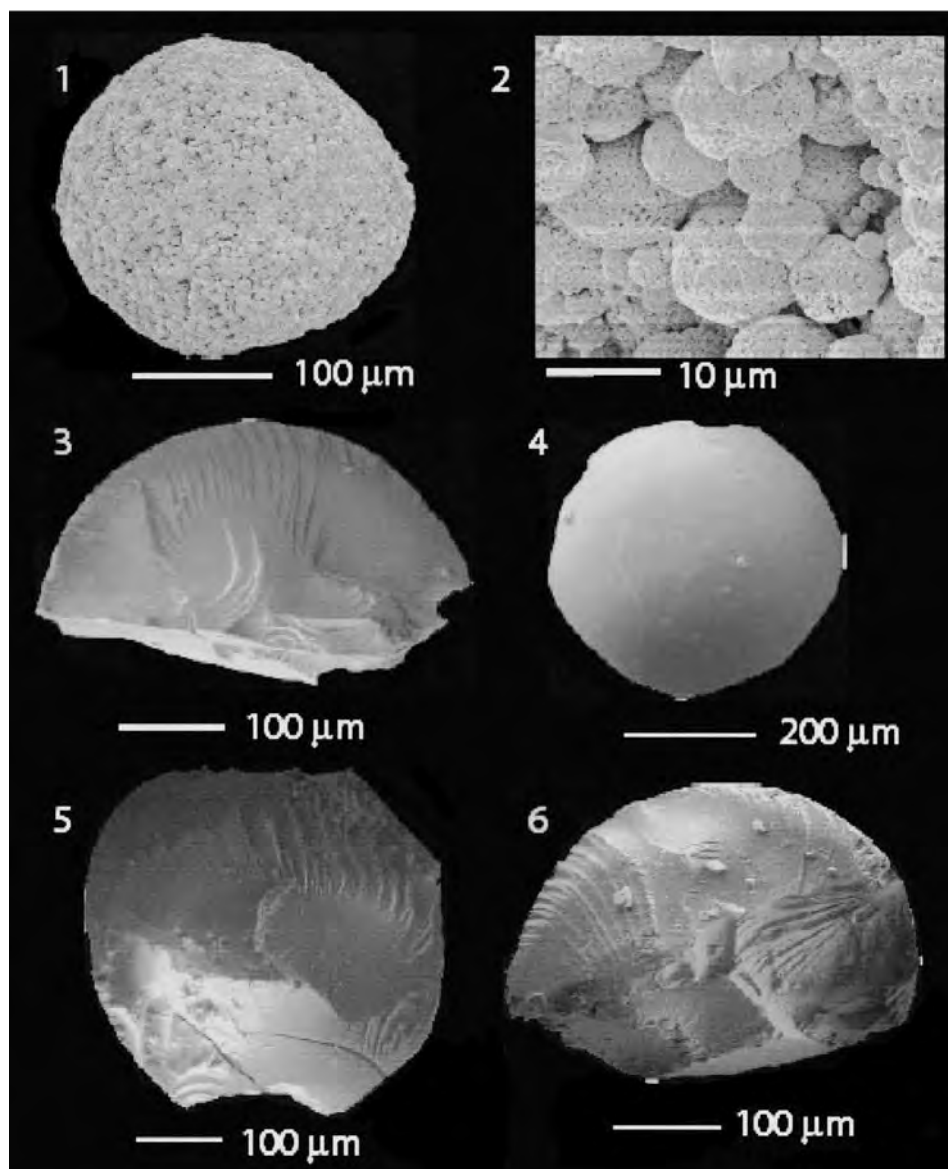
FIG. 5. – Spherules from the Mishor Rotem red layers. 1-2: Fe-rich spherule and surface detail from the K/T red layer and Ir anomaly. 3-4: translucent yellow amber spherules from the late Maastrichtian red marl layers showing conchoidal fractures and surface details. These spherules are glassy in appearance with smooth surfaces. The chemical composition is almost pure carbon (~ 90-95%), with some sulfur concentrated in the zoned outer rims.

FIG. 5. – *Sphérules des couches argileuses rouges de la coupe de Mishor Rotem.* 1-2 : *sphérules enrichies en fer observées dans la couche argileuse rouge de la limite K/T.* 3-4 : *sphérules d'ambre, translucides jaunes, observées dans les couches rouges du Maastrichtien tardif montrant des cassures conchoïdales. Ces sphérules ont un aspect vitreux et arrondi. Elles sont, au niveau de leur composition chimique, presque exclusivement composées de carbone (90-95 %), avec un peu de souffre concentré sur les bords externes.*

spherules, coinciding with high amounts of rounded glauconite grains at the base of the red layers, reflects the highly condensed sedimentation in this interval and accumulation by winnowing currents. Amber deposits of lower Cretaceous age have been reported from Lebanon, Jordan, Syria, as well as to the south on the Arabian-African continent, where they reflect the presence of densely forested areas under hot subtropical climate conditions [Dietrich, 1976; Wolfart, 1967; Azar *et al.,* 1999; Bandel *et al.,* 1997]. The Mishor Rotem amber spherules may be reworked from such deposits. However, due to their excellent preservation, these amber spherules do not result from the reworking of these lower Cretaceous amber deposits. During the late Maastrichtian, northeastern areas (Lebanon, Jordan and Syria) must have consequently similarly been forested and amber has been recovered. The source of the amber is assumed to be from a conifer belonging to the Araucariaceae, which grow in a tropical to subtropical nearshore environments (Weitschaft W., written communication). Clay mineralogy indicates that such conditions also prevailed during the late Maastrichtian at Mishor Rotem.

PLATINUM GROUP (PGE) AND TRACE ELEMENTS

Variations in geochemical phases of elements such as, Ti, K, Rb, and Zr related to terrigenous input versus Ca, Mg and Sr related to biogenic productivity, are excellent tools for interpreting paleoenvironmental changes in sedimentary successions with relatively low diagenetic overprints [Stueben *et al.,* 2002; Andreozzi *et al.,* 1997]. These criteria are also useful in identifying sea-level fluctuations, proximal-distal trends and especially intervals of condensed sedimentation in which elements of terrigenous origin are concentrated [Jarvis *et al.,* 2001]. The latter is used here to evaluate the cosmogenic (impact) and/or terrigenous (volcanism) origin of PGE. For example, if trace elements that are mainly bound to the lattice of minerals of terrigenous origin, such as Al, Ti, K, Rb, and Zr, show similar abundances as PGEs then the latter must have slowly accumulated during a period of reduced sedimentation and do not reflect additional input due to an impact or volcanism. Mg, Ca, Sr are generally incorporated into biogenic carbonates [Tucker

and Wright, 1990] and can be used as temperature proxies, because Mg and Sr incorporation into biogenic calcite is controlled by a temperature dependent physiological process [Smith *et al.,* 1994]. However, Mg and Sr can be also bound to mafic terrigenous minerals or clay minerals. Mn tends to be absorbed on organic matter and biogenic carbonate [Jarvis *et al.,* 2001], whereas barium may precipitate as sulfate from the water column or be incorporated in clay minerals.

Iridium and 18 other elements were determined by ICP-MS and X-ray fluorescence spectrometry from 30 samples spanning late Maastrichtian chalks, limestones, red marls and the K/T boundary at the Mishor Rotem section in order to differentiate the four red layers (RL-1 to RL-4) and determine their origins. The results show strong Pt and Pd anomalies in red layers RL-1 and RL-2, and Ir, Ru and Rh anomalies at the K/T boundary (fig. 6). In addition, RL-1 has element concentrations in all analyzed elements, except CaO and MnO (fig. 7). Much lower concentrations are observed in RL-4 at the K/T boundary and in RL-2. RL-2 shows no anomalous element concentrations compared with chalks and limestones, suggesting that deposition may be the result of reworking from the older RL-1. Zr and Rb are markers for detrital sedimentation and are clearly enriched together with Cu and Zn in RL-1 and slightly enriched in RL-4 at the K/T boundary, whereas in RL-2 and RL-3 no enrichments of these elements could be observed. Ba is enriched at the top of the RL-1 and just below the base of RL-4 at the K/T boundary. Sr increases significantly in RL-1 and to a lesser extent in RL-2 and 3. This implies that this element is not only linked with Ca (calcite) but also to terrigenous minerals and therefore its ratio with Ca cannot

be used to infer paleo-temperatures. Good correlations (R^2 0.8) link Rb, Zn, Zr, La, Cu and Fe, which show the same strong negative correlation with Ca (R^2 0.9) and Mn (R^2 0.7) reflecting a terrigenous origin for the former. The absence of a significant correlation with Sr ($R^2 = 0.5$-0.6) confirms that this element maybe linked either to carbonate or detrital minerals.

PGE anomalies in sediments may result from an enriched element source (cosmic or mantle-type material), from changes in the sedimentary environment, including concentration from seawater into a reducing sedimentary environment and removal at redox boundaries within sediments, or from sediments enriched in organic matter or sulphides [Kramar *et al.,* 2001; Barnes *et al.,* 1985; Kyte and Wasson, 1986; Pfeifer *et al.,* 1997]. The PGE and trace metal data show two clear anomalies in CF1 plus one anomaly mainly enriched in PGEs (especially Ir) at the K/T boundary (figs 6, 7). The chondrite normalized PGE patterns of RL-1 and RL-2 show increasing values from Ir to Pd (Pt/Ir = 3.6 and 4.7; Pd/Ir = 44 and 49) indicating a terrigenous or volcanogenic enrichment (fig. 8). Thus an extraterrestrial origin in these samples appears improbable. The enrichment of Rb, Zr and Zn in RL-1 may indicate increased detrital input, reduced biogenic sedimentation, or volcanogenic influx. The missing enrichment of terrigenous elements in RL-2 and RL-3 may indicate reworking from RL-1 and suggests that the PGE anomaly is diagenetically enriched. The relatively low Fe content (5%) in the three red layers (RL-1 to RL-3) argues against drastically changing redox conditions.
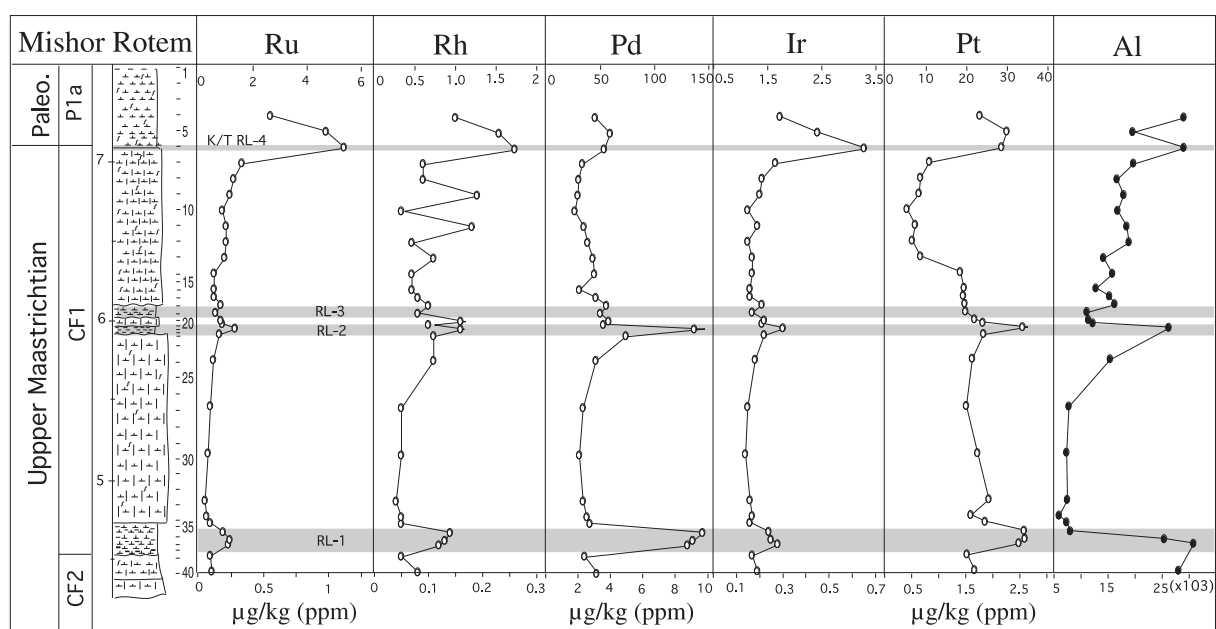

FIG. 6. – Platinum Group Element (PGE) distribution across the late Maastrichtian red layers and K/T boundary. Note the Ir, Ru and Rh enrichments in the boundary red clay layer and Pd, Pt and Al enrichments in red layers one and two.
FIG. 6. – *Distribution des éléments du groupe du platine (EGP) dans l'intervalle allant des couches argileuses rouges du Maastrichtien tardif jusqu'à celle de la limite K/T. Il faut souligner que les proportions de Ir, Ru et Rh augmentent dans la couche limite K/T, alors que les taux de Pd, Pt sont plus importants dans les couches argileuses rouges un et deux.*
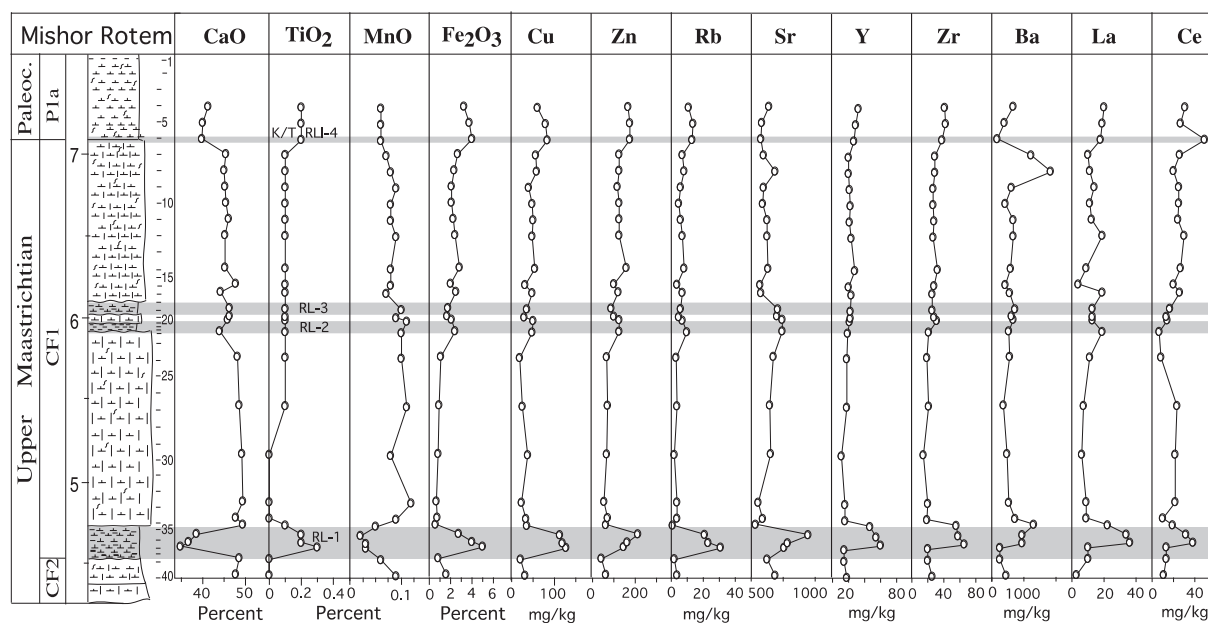
FIG. 7. – Trace element distribution across the late Maastrichtian and K/T boundary red layers. Note lowermost red layer is enriched in all trace elements, but this is not the case for red layers 2 and 3, or the K/T red layer.

FIG. 7. – *Distribution des éléments-traces dans l'intervalle allant des couches argileuses rouges du Maastrichtien tardif jusqu'à celle de la limite K/T. Il faut souligner que ces éléments-traces augmentent dans la couche argileuse rouge basale 1 ; cet accroissement en éléments rares n'est pas observé dans les couches argileuses rouges 2 et 3 et à la limite K/T.*

The RL-4 anomaly at the K/T boundary is clearly different in origin and shows a flat, roughly chondritic PGE pattern (Pt/Ir = 1.6; Pd/Ir = 4.8) with higher concentrations of Ir, Ru and Rh, and lower concentrations of Pd compared to the anomalies in RL-2 and RL-1 (fig. 6, 8). This anomaly can probably be linked to the impact at the K/T boundary. The increase in terrigenous elements at and above the K/T boundary is evident when compared with the decreased biogenic productivity after the K/T boundary, but it is not as strong as in RL-4.

Geochemical proxies thus demonstrate that Ir enrichments are not necessarily linked to impact events. Small Ir anomalies, such those observed in RL-4, RL-3 and RL-2, can result from higher terrigenous (volcanogenic) input and/or reduced sedimentation rates and must be critically evaluated within the context of the overall PGE and traces elements distribution pattern to decipher its origin.

MINERALOGY

Bulk rock mineralogy

In the Mishor Rotem section, sediments are generally dominated by calcite (60-95%) and phyllosilicates (5-38%) with minor quartz (0.5-3%), and sporadic occurrences of K-feldspar (0-1.5%), plagioclase and goethite (fig. 9). At the CF2-CF3 transition the calcite decreases from 85-90% in three minima that coincide with increased phyllosilicates (up to 40%). Because these calcite minima do not correspond to increased quartz and feldspar, they probably reflect dissolution rather than increased detrital input. In the upper CF2 and lower CF1 intervals calcite is high (up to 92%) to the detriment of quartz and phyllosilicates, but in the red layer (RL-1), quartz (3%) and K-felspar (1.5%) and

phyllosilicates (30%) increase and calcite decreases (66%). In contrast, red marl RL-2 and RL-3 show no increase in detrital components. No minerals indicative of nearby volcanic activity (e.g. amphibole, pyroxenes) have been detected in any of the red marl layers. Above RL-2 and RL-3, quartz and calcite decrease with a corresponding increase in phyllosilicates. No major change is observed at the K/T transition because most of the boundary interval is missing
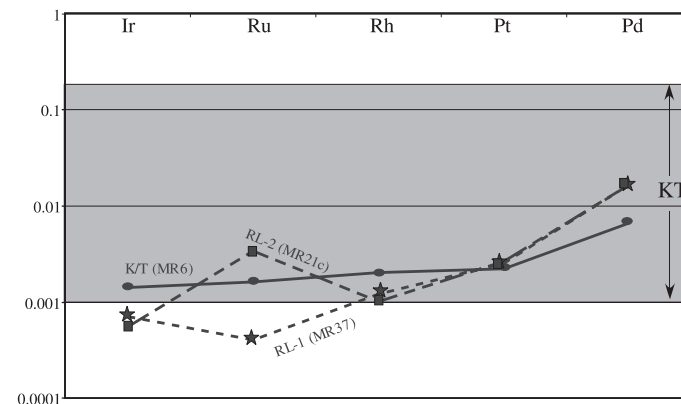

FIG. 8. – Chondrite-normalized PGE patterns from Red layers 1 (MR37), 2 (MR21c) and RL4 (KT boundary, sample MR6). Note that only K/T PGEs show characteristic patterns of the boundary impact event. PGE patterns of RL1 and RL2 show increasing values from Ir to Pd indicating terrigenous or volcanogenic enrichment. The RL4 anomaly (K/T boundary) differs in that it displays a flat chondritic PGE pattern with higher Ir, Ru and Rh.

FIG. 8. – *Distribution des EGP normalisés (chondrite) des couches rouges 1 (MR37), (MR21c) et RL4 (limite KT, échantillon MR6). Il faut souligner que seuls les EGP de la limite K/T montre une distribution caractéristique d'un impact. Les EGP des couches RL1 et RL2 augmentent de Ir à Pd indiquant une origine volcanique. L'anomalie du niveau RL4 (limite K/T) est différente, sa distribution étant plus plate, chondritique avec des teneurs en Ir, Ru et Rh plus élevées.*
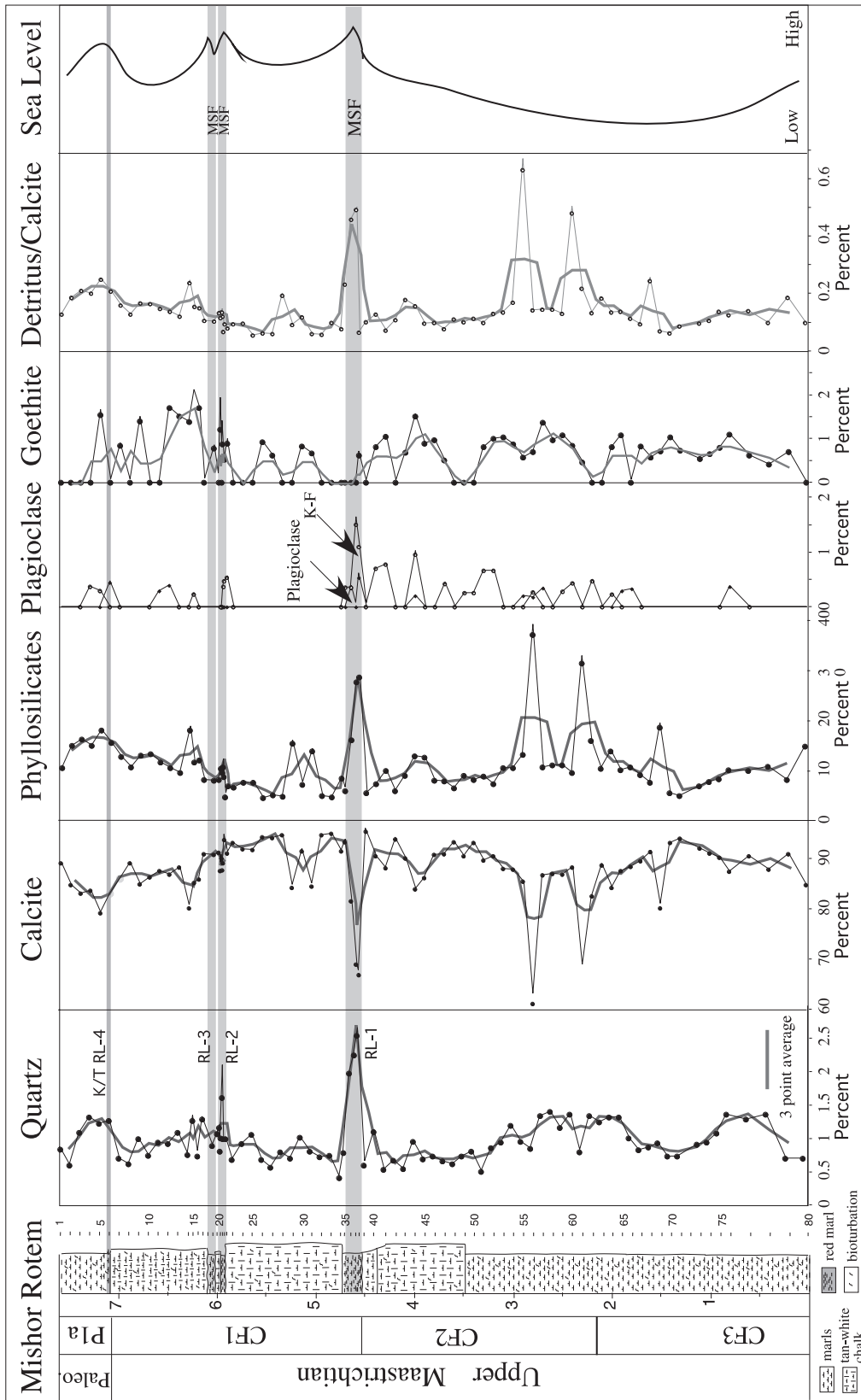
FIG. 9. – Bulk rock composition at Mishor Rotem. The label detritus include quartz, plagioclase, K-feldpar and phyllosilicates. The dominant sedimentary components are calcite and phyllosilicates with minor influx of quartz, K-feldspar, plagioclase and goethite. Note lowermost red clay layer is enriched in detrital minerals, contrary to RL-2 and 3. The long term increase in detrital components in the marly intervals correspond mainly to sea-level lowstands and increased continental runoff. Chalk intervals are characterized by decreased detrital input.

FIG. 9. – *Distribution des minéraux majeurs dans la coupe de Mishor Rotem. Sous le terme « détritique » ont été inclus le quartz, le plagioclase, le feldspath-K et les phyllosilicates. Les minéraux dominants sont la calcite et les phyllosilicates avec des quantités mineures de quartz, feldspath-K, plagioclase et goethite. Il faut observer que la couche argileuse rouge basale est enrichie en minéraux détritiques, contrairement aux niveaux RL-2 et RL-3. L'augmentation à long terme des composants détritiques dans les intervalles marneux correspond surtout à des périodes de bas niveau marin et à un important apport venu du continent. Les intervalles crayeux correspondent à une diminution de l'apport détritique.*

with only remnants of the boundary clay infilling the erosional surface of the underlying marly limestone.

Clay mineralogy (< 2 μm)

The < 2 μm clay fraction is composed of smectite, kaolinite, palygorskite, mica and chlorite. Kaolinite (35-60%) and smectite (30-50%) dominate the clay mineral fraction in the lowermost 3 m (fig. 10). Above this interval, kaolinite decreases gradually and smectite reaches a maximum of 50%. In the chalk of zone CF2 there is a significant increase in palygorskite (19%) along with chlorite (10%) and peak abundance of mica (37%) to the detriment of kaolinite and smectite. Smectite is dominant (40-50%) in RL-1 to RL-3, coincident with low kaolinite, increased palygorskite and chlorite in RL-2. The thin (2-3 cm) chalk layer between RL-2 and RL-3 shows a strong decrease in smectite (from 41 to 19%), and increase in kaolinite and palygorskite. Smectite and kaolinite dominate the clay fraction in the upper part of CF1, with low palygorskite and mica contents, similar to the lower part of CF3.

Ratios of smectite/illite + chlorite + palygorskite (SM/(I + C + P), smectite/kaolinite (SM/K) and smectite/ other clays (SM/RC) all show similar trends. The section can be subdivided into 6 parts: (1) a marly lower interval (0-3.5 m), where smectite and kaolinite dominate; (2) a lower chalk interval (3.5-4.5 m) with decreased smectite and kaolinite and increased palygorskite, mica and chlorite; (3) the lower part of the chalk layer in CF2 (4.7-5.5 m) characterized by high smectite, palygorskite and mica and low kaolinite; (4) the upper part of the chalk in CF1 (5.5-5.90 m) with decreased smectite and palygorskite and increased kaolinite; (5) the marly limestone above RL-3 (6.25-6.75 m) marked by high smectite and increasing kaolinite and low palygorskite and mica, and (6) the uppermost part of the Maastrichtian with decreasing smectite and increasing kaolinite (fig. 10).

DISCUSSION

Clay minerals as climate and environmental proxies

Clay mineral assemblages reflect continental morphology and tectonic activity, as well as climate evolution and associated sea-level fluctuations [Chamley, l989, 1997; Weaver, l989; Li *et al.,* 2000; Adatte *et al.,* 2002]. Illite and chlorite are considered common byproducts of weathering reactions with low hydrolysis typical of cool to temperate and/or dry climates.

Palygorskite

This mineral has three main origins: (1) production *in situ* as result of hydrothermal weathering of Mg-bearing rocks, particularly of volcanic origin, combined with the influence of sea water [Karpoff *et al.,* 1989]. This type of hydrothermal activity appears to be absent in the studied area during the Upper Maastrichtian; (2) palygorskite may form along coastal and peri-marine environments where continental alkaline waters are concentrated by evaporation. Such Mg- and Si-rich brines favor the precipitation of palygorskite and/or smectite [Robert and Chamley, 1991; Pletsch, 1996; Bolle and Adatte, 2001], particularly under warm

temperatures; (3) palygorskite can also form on land in calcrete soils under arid conditions [Chamley, 1989; Robert and Chamley, 1991]. The existence of restricted shallow Maastrichtian-Paleocene syncline basins favorable to the neoformation of palygorskite in southern Israel [Arkin *et al.,* 1972; Almogi-Labin *et al.,* 1990] suggests that most of this fibrous clay may have formed locally in shallow coastal basins during periods of arid warm climates, particularly in the uppermost part of zone CF2 and lower part of CF1 (fig. 10).

Kaolinite

This mineral is generally a byproduct of highly hydrolytic weathering reactions in perennially warm humid climates and its formation requires a minimum of 15°C [Gaucher, 1981]. During deposition in zone CF3, dominance of smectite and kaolinite over chlorite, mica and palygorskite indicates that seasonal to humid conditions prevailed in the source area and/or a sea-level highstand (figs 9-10). In the lower part of CF2, increased kaolinite, decreasing smectite and nearly constant low mica and palygorskite, and low chlorite indicate more humid wet conditions that coincide with a lower sea-level. Although increased kaolinite may reflect humid conditions as well as increased erosion during low sea levels, the latter is not the case because there is no strong coeval input of other detrital clay minerals (e.g. mica, chlorite). This interpretation is consistent with a study of Arkin *et al.* [1972] who considered the presence of kaolinite in Maastritchtian-Danian sediments of the southeastern part of the Negev to be a climatic indicator. The source of kaolinite was probably a land mass located to the east-southeast (Arabian-Nubian continent), which had a moderate relief and a well developed soil cover [Arkin *et al.,* 1972].

Smectite

The presence of abundant smectite is generally linked to transgressive seas and warm climate with alternating humid and arid seasons, but can also reflect volcanic activity [Chamley, 1989, 1997; Deconinck, 1992]. The origin and deposition of smectite depends on several factors. During a sea-level rise, smectite is reworked from soils and enriched by differential settling in open environments. Chlorite, kaolinite and mica are deposited close to shorelines, while smectites are transported away from shores [Gibbs, 1977; Adatte and Rumley, 1989]. Increased smectite therefore reflects sea-level highstand periods [Chamley *et al.,* 1990] whereas increased kaolinite, chlorite and mica suggest lowstand periods. Abundance of detrital smectite inherited from soils and exported to the open ocean during high sea-levels, reflects extended low relief land areas characterized by a hot climate and seasonal changes in humidity [Chamley, 1989, 1997].

Submarine alteration of volcanic or impact glass and ash is frequently invoked to explain the widespread occurrence of smectite that is often associated with zeolites (clinoptilolite) and opal-CT in marine environments [Weaver and Beck, 1977], especially during the Cretaceous, which was a period of extensive sea level rise linked to high spreading rates and volcanism. A global increase in volcanism coincident with a high sea-level and consequently flooding of
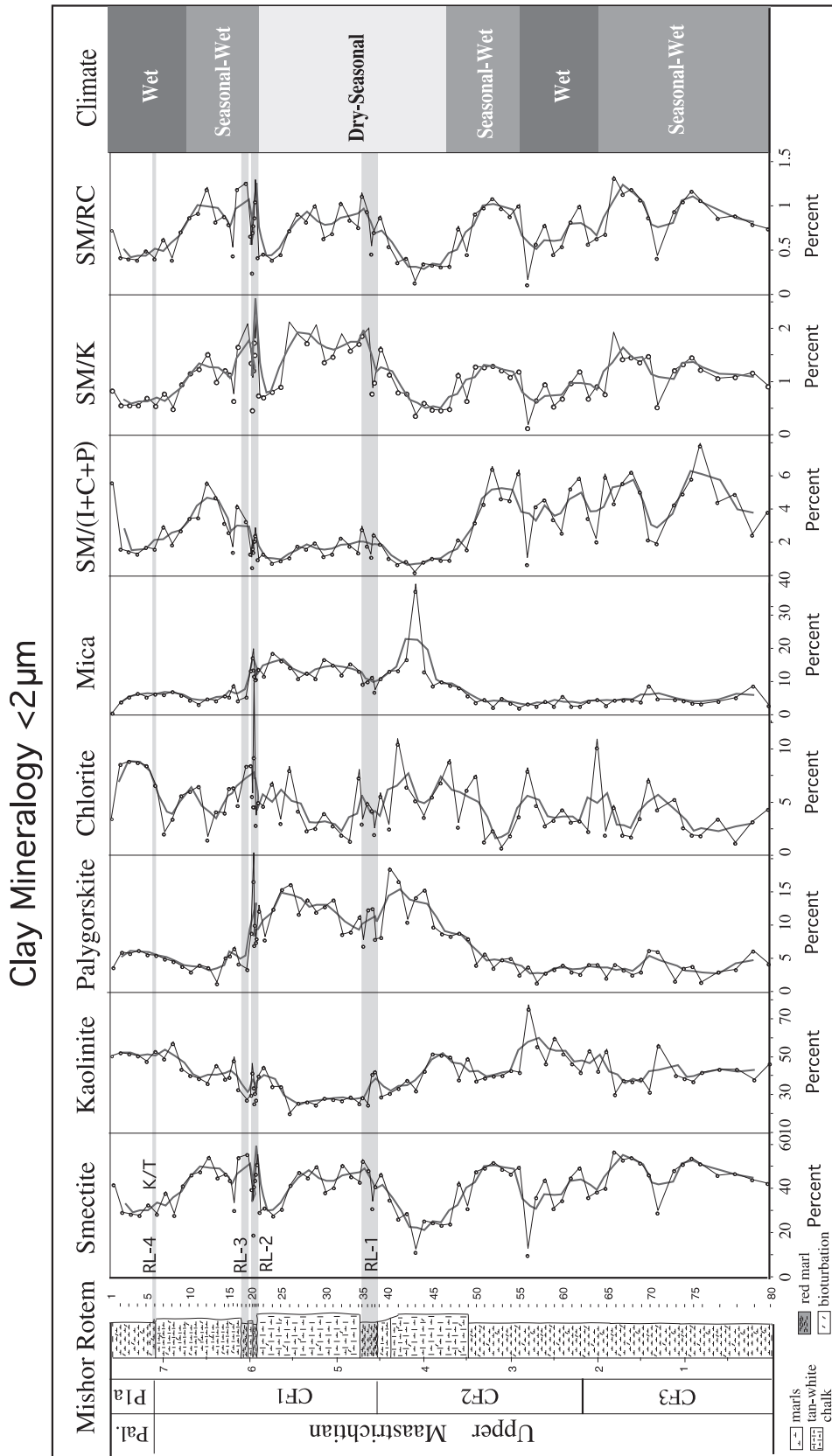
FIG. 10. – The < 2 µm clay mineral composition (relative percent) and smectite/mica + chlorite + palygorskite (SM/I + C + P), smectite/kaolinite (SM/K) and smectite/other minerals (SM/RC) ratios (counts by seconds) at Mishor Rotem. Note that smectite and kaolinite are most abundant, followed by mica, chlorite, and palygorskite and reflect a paleoclimate fluctuating from wet to seasonal dry conditions. Chalk deposition occurred under drier conditions as indicated by the highest amount of palygorskite and lowest kaolinite.

FIG. 10. – *Evolution de la composition des minéraux argileux (MA) de la fraction < 2 µm (en % relatifs) et des rapports smectite/mica + chlorite + palygorskite (SM/I + C + P), smectite/kaolinite (SM/K) and smectite/autres minéraux (SM/RC), en coups par seconde dans la coupe de Mishor Rotem. Smectite et kaolinite sont les MA les plus abondants suivies par le mica, la chlorite et la palygorskite, indiquant un paléoclimat fluctuant de conditions humides vers un climat plus sec et saisonnier. Les dépôts de craie correspondent à des conditions plus arides, comme l'attestent les quantités élevées de palygorskite, au détriment de la kaolinite.*

land areas is therefore a major contributing factor to the enrichment of smectite in marine conditions [Thiry and Jacquin, 1993].

The detrital smectite deposited along the eastern Tethyan margin could be derived partly from argillized submarine volcanic rocks [Shoval, 2000]. Authigenesis from sea-water of smectite seems unlikely, because it does not explain the variations and the disappearance of detrital clays during times of high or low sea-levels. Diagenetic alteration of clays is also unlikely because Tertiary deposits in the Negev do not exceed 500-1000 m [Bolle and Adatte, 2001] and hence clay minerals (e.g. smectites) did not suffer deep burial diagenesis, which occurs at depths exceeding 2 km [Chamley, 1997]. Absence of diagenetic overprints due to burial diagenesis is indicated by (1) the constant but variable amounts of smectite, (2) the co-existence of smectite with high amounts of kaolinite and palygorskite, and (3) the near absence of mixed layered illite-smectite (fig. 10). In this study, detrital input is therefore the dominant factor for clay mineral distributions in marine sediments.

Kaolinite/smectite (K/SM)

The K/SM ratio is a climate proxy that reflects humid/warm to more dry and seasonal climate variations [e.g. Robert and Chamley, 1991; Robert and Kennett, 1992], and can therefore be used as proxy for climate change (fig. 10). Since kaolinite is usually more abundant in coastal areas and smectite in open marine environments, the K/SM ratios may also reflect sea-level changes. But primarily, variations in K/SM ratios are linked to climate changes. In the same way, the smectite/(illite + mica + palygorskite) or SM/(I + C + P) ratio reflects fluctuations from seasonal to more arid conditions under which palygorskite is preferentially formed and both mica and chlorite are physically eroded.

Smectite as proxy for impact or volcanic glass

Smectite may also derive from impact glass alteration [Ortega-Huertas *et al.,* 2002]. Debrabant *et al.* [1999] noted such smectites at El Caribe in Guatemala and in central Mexico based on XRD and thermoanalytic (DTA) techniques and interpreted them as Na-Mg bentonite (Cheto type) derived from the weathering of a spherule-bearing layer linked to the Chicxulub impact. Keller *et al.,* [2003a,b] reported the same type of smectite from glass spherule deposits of Belize and southern Mexico. Although these Cheto Mg-smectite clays are commonly interpreted as weathering products of glass linked to the Chicxulub impact, Elliot *et al.* [1989] and Elliot [1993] noted that they may also be derived from volcanic glass.

Cheto smectites are characterized by excellent crystallinity, high intensity of the 001 reflection and constitute the main or even exclusive part of the clay mineralogic assemblage in Central and North America. In contrast, at Mishor Rotem the clay fraction does not exceed 60% and is poorly crystallized, suggesting reworking from soils enriched by differential settling during a sea level rise. Smectite is enriched in the red clay layers (fig. 10), which coincide with high sea levels (MSF). An impact glass origin therefore appears unlikely, though some part of the smectite content may have derived from volcanic glass alteration, as suggested by the PGE and trace elements distributions.

Climate and sea level changes

Variations in the bulk rock and clay mineral compositions reflect major sea level and climate changes during the late Maastrichtian in the eastern Tethys. During the upper part of zone CF3, increased calcite, smectite and high K/SM ratios, but low phyllosilicates, quartz, feldspar, palygorskite and kaolinite suggest a high sea-level and seasonally wet climate (figs 9-10). A lower sea level and wet climate are indicated in the uppermost part of zone CF3 and lowermost part of CF2 by decreased calcite, smectite and K/SM ratio, but increased quartz, phyllosilicates, detritus/calcite, and kaolinite. In the middle of zone CF2 (3.0-3.5 m) increased smectite marks the re-establishment of more seasonally wet conditions and corresponds to a sea level rise (fig. 10). In the overlying chalk of the upper zone CF2, the pronounced decrease in quartz, smectite, decrease in kaolinite and increase in palygorskite, mica and chlorite, reflect increased sea level but dry warm climate associated with seasonal aridity, enhanced evaporation and weakened leaching of adjacent land areas and coastal basins.

The subsequent deposition of the first red marl layer (RL-1) near the base of CF1 occurred during this type of dry seasonal climate and high sea level and is interpreted as a maximum flooding surface (MSF) characterized by low sediment accumulation, decreased calcite and increased detrital inputs. The presence of well rounded glauconite grains, suggest current winnowing, probably enhanced by the paleolocation of the Mishor Rotem section on an anticline. Warm seasonal-arid conditions and high sea level prevailed during the lower part of CF1 as indicated by high smectite and palygorskite and lower kaolinite. The presence of well-crystallized mica, high K-feldspar and plagioclase indicate a weakened hydrolyzing process in the source area. The two closely spaced red marl layers (RL-2, RL-3) in the middle of CF1 are less enriched in detrital components and glauconite, which suggests lower magnitude sea level fluctuations (4-5th order) perhaps linked to regional tectonic activity. Trace and PGE elements strengthen these observations (figs 6, 7) because they show maximum concentrations in RL-1 and decreasing concentrations in RL-2 and RL-3. Above the red marl layers in the upper zone CF1, the decrease in palygorskite and mica to the benefit of smectite and kaolinite marks the re-establishment or more seasonal to wet conditions.

More humid wet conditions prevailed in the uppermost zone CF1 and early Danian, as indicated by dominant kaolinite, decreased smectite, low palygorskite and mica contents. However, the eustatic sea level rise that marks the end of the Maastrichtian, K/T boundary and earliest Danian [Hardenbol *et al.,* 1998; Adatte *et al.,* 2002a] is not evident in the Mishor Rotem section probably because the uppermost Maastrichtian (uppermost CF1) and lowermost Danian (P0, Pla(l)) is missing due to a hiatus. However, in addition to the eustatic signal, Negev sections may also record local variations resulting from tectonic activity of the Syrian arc folding phase [Flexer *et al.,* 1986]. Paleogeographically, the Negev was located close to the ophiolite belt of the Syrian-Turkey arc (fig. 1) which became active during the Maastrichtian [Almogi-Labin *et al.,* 1990, 1993]. Sedimentation in the Maastrichtian and its numerous lithological breaks and hiatuses reflect partly the transition from a relatively stable passive tectonic province to a mobile and active phase. This part

of the Tethys ocean was therefore strongly reduced during the Maastrichtian and consequently marked significant tectono-eustasic changes (in ocean basin volume) which appear to be recorded in Negev sedimentary deposits. Similar climatic trends for the late Maastrichtian have been observed at a nearby Negev section (Ben Gurion) [Bolle *et al.,* 2000], as well as in Tunisia [Adatte *et al.,* 2002], Italy (Gubbio) [Robert and Chamley, 1990] and South Atlantic (Walvis Rigde) [Robert and Chamley, 1990]. These climatic changes may be linked to a greenhouse effect induced by Deccan volcanism.

Biotic Effects

Global climate changes coupled with regional intermittent high stress conditions very likely account for the low species richness, anomalous peaks in *Guembelitria* and the very low abundance of keeled globotruncanids (figs 4, 11) that appear to be particular to the eastern Tethys (e.g. Israel, Egypt). In central Egypt, planktic foraminiferal assemblages indicate even higher stress conditions in the late Maastrichtian than in southern Israel, as suggested by lower species richness and *Guembelitria* blooms that dominate (75-90%) the foraminiferal populations. At times of improving conditions the low oxygen tolerant heterohelicids thrive. The constant high presence of this group in the Mishor Rotem section and the lower abundance of *Guembelitria* indicates less biotic stress in Israel. In Egypt, the high stress assemblages are accompanied by strongly negative $\delta^{13}C$ values that suggest a breakdown of the surface-to-bottom gradient of the $^{13}C/^{12}C$ ratio [Keller, 2002]. This breakdown in primary productivity began during global climate cooling in CF3 and a sea level regression that peaked at 65.5 Ma, but continued also during the global warming in zone CF1.

A possible cause for the high biotic stress conditions in central Egypt is a low sea level which may have restricted circulation and intermittently created stagnant eutrophic basin conditions, eliminating specialist and most generalist species and promoting blooms of *Guembelitria* [Keller, 2002]. However, the *Guembelitria* blooms in Israel are coeval and indicate more widespread biotic effects related to oceanographic conditions external to Egypt. Recently, coeval *Guembelitria* blooms have been observed in the Indian Ocean on Ninetyeast Ridge DSDP Site 216 in association with mantle plume volcanism [Keller, 2003]. This suggests that the late Maastrichtian high stress conditions in Israel and Egypt may be linked to mantle plume and hotspot volcanism in the Indian Ocean. The volcanic influx indicated by geochemical data is thus also causing high environmental stress.

PGE anomalies : volcanism, impact or reduced sedimentation ?

There is increasing evidence that the end-Cretaceous experienced multiple impacts (comet shower), rather than a single large impact as generally hypothesized [Keller *et al.,* 2003a]. In addition, there is increasing evidence that the Chicxulub impact predates the K/T boundary, as indicated by impact ejecta layers interbedded in late Maastrichtian marls in northeastern Mexico. A pre-K/T age is also indicated by late Maastrichtian limestones of paleomagnetic chron 29R overlying the impact breccia in the new Yaxopoil-1 core drilled within the Chicxulub crater [Keller *et al.,* 2004]. The reported multiple glass spherule layers in the Mishor Rotem sec-

tion of Israel by Rosenfeld *et al.* [l989] suggested further evidence of multiple impact events. The results of this study confirm evidence for a K/T boundary impact, with typical Ir anomaly and low Pd, but not for the three late Maastrichtian red clay layers. In these red layers the ratio between Ir, Pt and Pd elements and the distribution of trace elements indicate a terrigenous/volcanogenic origin (high Pd, minor Ir). The absence of typical weathered glass products, such as Cheto smectite, also supports these findings. The red clay layers appear to have been deposited during high sea-levels on topographic highs.

Elwood *et al.* [2003] reported two impacts based on Ir anomalies, increased Ni, Cr, As and Zn contents and small iron microspherules from a K/T section in the Abat Basin, Oman. They interpreted one anomaly to represent the K/T boundary and the second, about 1 m below, a late Maastrichtian impact. But in the absence of other PGE data, an impact origin of the Ir enrichments cannot be ascertained with confidence. The stratigraphic occurrences of these two Ir enrichments are surprisingly similar to the Mishor Rotem section. In both localities they are associated with hard-grounds suggesting intervals of reduced sedimentation and/or hiatuses [Le Callonec *et al.,* 1998]. Moreover the coincidence of increased Zn may indicate increased accumulation of terrigenous-volcanogenic elements due to reduced sedimentation similar to the red layers at Mishor Rotem. The described microspherules from the Ir enriched levels are also quite similar, consisting of goethite and glauconitic spherules, which are not definitive criteria for an impact event since they may form by diagenetic replacement. Goethite and glauconite concentrations are typically formed on condensed surfaces during sea level trangressions in open marine environments. Increased Ni, Cr and As are often linked to the presence of these minerals. Without biostratigraphic or further geochemical information, we therefore assume that the Ir enrichments reported by Elwood *et al.* [2003] are equivalent to the red layers below the K/T boundary at Mishor Rotem.

At Mishov Rotem, the stratigraphic position of the red layers 1, 2 and 3 coincide with the onset intensive (Deccan) volcanic activity as also suggested by the high stress faunal assemblages and their correlation with Indian Ocean Ninetyeast Ridge mantle plume volcanism (fig. 11). Another potential source of volcanic activity may be the ophiolite belt of the Syrian-Turkey arc, which became active during the Maastrichtian [Almogi-Labin *et al.,* 1990]. Within this context, the Pd dominated PGE observed in the uppermost Maastrichtian red-layers are likely of volcanic origin and accumulated with other terrigenous elements in condensed intervals linked to sea level transgressions.

CONCLUSIONS

Mineralogical, geochemical, stratigraphic and faunal data of the late Maastrichian-early Paleocene of the Mishor Rotem section reveals a complex inter-relationship between changes in sea-level, paleoclimate, tectonism, volcanism, impacts and biotic effects. The following conclusions can be reached.

1) PGE anomalies from 4 different red clay layers appear to have different origins. The late Maastrichtian zone CF1 red layers (RL-1, 2, and 3) are dominated by Pd PGE anomalies which coincide with increased trace elements of terrigenous and volcanogenic origins. These three clay layers are linked
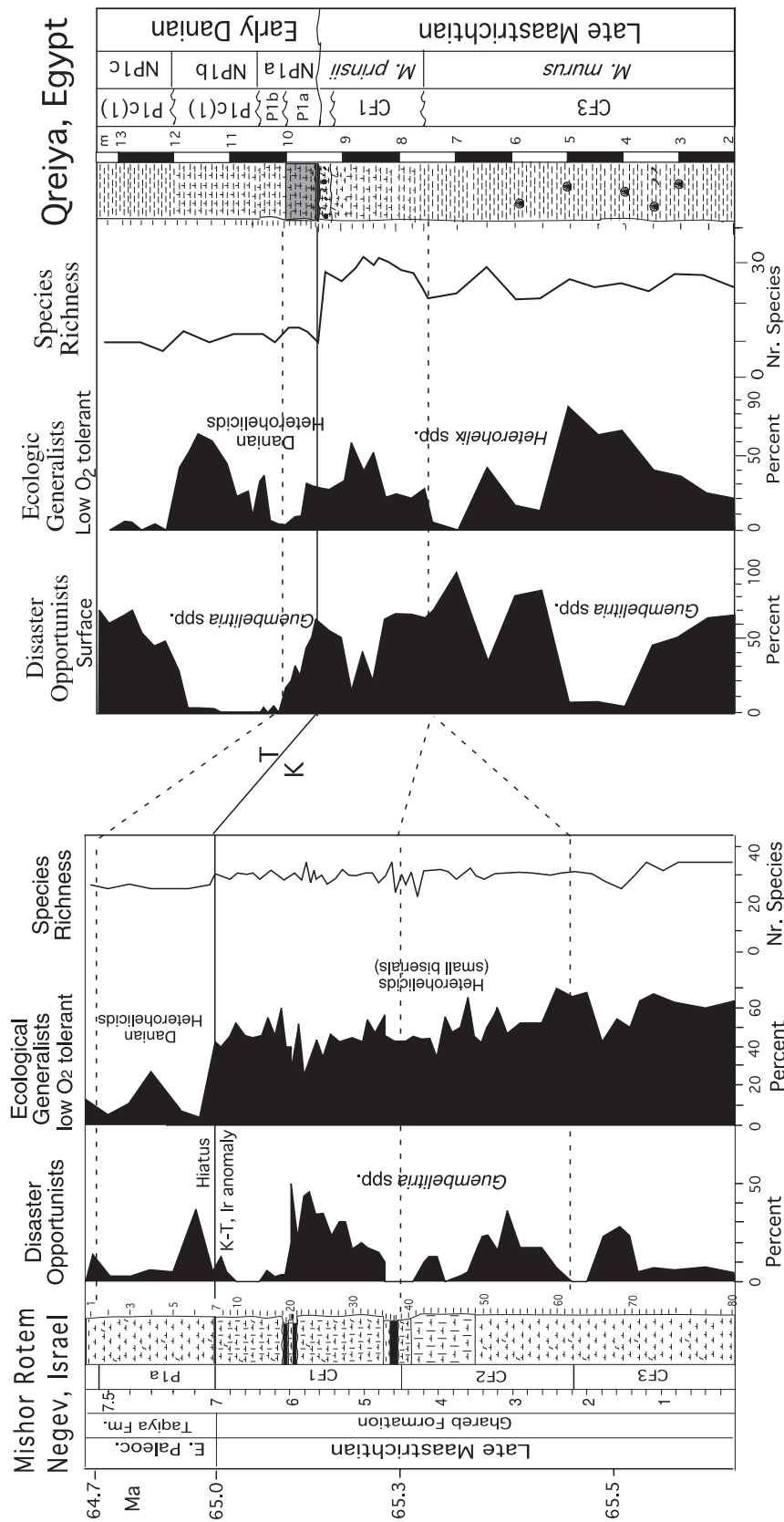
Fig. 11. – Disaster opportunist *Guembelitria* blooms at Mishor Rotem can be correlated with similar, though larger blooms in Egypt. The greater intensity of the blooms in Egypt and alternating *Guembelitria/Heterohelix* populations indicate that the biotic stress levels in Egypt were greater than in Israel. Coeval *Guembelitria* blooms in the Indian Ocean are associated with mantle plume volcanism and reveal the catastrophic biotic effects of volcanism over wide geographic regions.

Fig. 11. – *Corrélation des proliférations des genres oportunistes* Guembelitria *dans la coupe de Mishor Rotem avec des proliférations similaires quoique plus importantes observées en Egypte. Les blooms, plus intenses, observés en Egypte et l'alternance des populations de* Guembelitria *et d'* Heterohelix *indiquent un stress biologique plus élevé en Egypte qu'en Israel. Des blooms contemporains ont été aussi observés dans des coupes localisées dans l'océan Indien associées à du volcanisme lié à un point chaud, reflètant des effets biologiques catastrophiques liés à ce genre de volcanisme, et ceci sur une aire géographique considérable.*

to increased Deccan or Syrian-Turkey arc volcanism and may be regionally correlated with similar PGE enrichments in Oman. The K/T boundary red layer (RL-1) is characterized by an Ir dominated PGE anomaly and implies an impact source. All four red clay layers appear to have been deposited on topographic highs during high sea-levels and low sedimentation rates.

2) We observed translucent yellow and darker amber spherules, which were probably derived from forests. Glauconite is common and goethite spherules are mostly present in the K/T red layer. We could not confirm the presence of silica-rich microspherules reported by Rosenfeld *et al.* [1989]. The absence of typical weathering glass products, such as Cheto smectite, indicates that no glass altered clays are present.

3) Litho- and biostratigraphy, geochemistry and mineralogy suggest repeated sea-level and climatic fluctuations ranging from seasonally wet climate in the upper part of CF3, to more arid conditions coinciding with chalk deposition (upper CF2-lower CF3) and the reestablishment of more humid wet conditions in the uppermost zone CF1 and early Danian.

4) In addition to the global eustatic signal, Negev sections may also record local variations resulting from tectonic activity of the Syrian arc folding phase. Sedimentation in the Maastrichtian and its numerous lithological breaks and hiatuses reflect partly the transition from a relatively stable passive tectonic province to a mobile and active phase. This part of the Tethys ocean was therefore strongly reduced during the Maastrichtian and consequently marked significant tectono-eustasic changes (in ocean basin volume) which appear to be recorded in Negev sedimentary deposits.

5) Planktic foraminifera experienced relatively high stress conditions during the late Maastrichtian as indicated by the low species richness and low abundance of globotruncanids. Times of more severe stress are indicated by the disaster opportunist *Guembelitria* blooms, which can be correlated to central Egypt and also to Indian Ocean localities associated with mantle plume volcanism. This supports the mineralogical and geochemical observations of volcanic influx and reveals the detrimental biotic effects of intense volcanism.

References

ABRAMOVICH S., ALMOGI L.A. & BENJAMINI C. (1998). – Decline of the Maastrichtian pelagic ecosystem based on planktic foraminifera assemblage change; implication for the terminal Cretaceous faunal crisis. – *Geology,* **26** (1), 63-66.

ADATTE T. & RUMLEY G. (1989). – Sedimentology and mineralogy of Valanginian and Hauterivian in the stratotypic region (Jura mountains, Switzerland). In: WIEDMANN J., Ed., Cretaceous of the western Tethys. – Proceedings *3rd International Cretaceous Symposium*. – Scheizerbart'sche Verlagsbuchhandlung, Stuttgart, 329-351.

ADATTE T., STINNESBECK W. & KELLER G. (1996). – Lithostratigraphic and mineralogic correlations of near K-T boundary clastic sediments in northeastern Mexico: implications for origin and nature of deposition. – *Geol. Soc. Amer., Sp. Paper*, **307**, 211-226.

ADATTE T., KELLER G. & STINNESBECK W. (2002). – Late Cretaceous to early Paleocene climate and sea-level fluctuations. – *Palaeogeogr., Palaeoclimatol., Palaeoecol.*, **178**, 165-196.

ALMOGI-LABIN A., FLEXER A., HONIGSTEIN A., ROSENFELD A. & ROSENTHAL E. (1990). – Biostratigraphy and tectonically controlled sedimentation of the Maastrichtian in Israel and adjacent countries. – *Rev. Esp. Paleontol.*, **5**, 41-52.

ALMOGI-LABIN A., BEIN A. & SASS E. (1993). – Late Cretaceous upwelling system along the southern Tethys margin (Israel): interrelationship between productivity, bottom water environments and organic matter preservation. – *Paleoceanography*, **8**, 671-690.

ALVAREZ L. W., ALVAREZ W., ASARO F. & MICHEL H. V. (1980). – Extraterrestrial causes for the Cretaceous-Tertiary extinction. – *Science*, **208**, 1095-1108.

ANDREOZZI M., DINELLI E. & TATEO F. (1997). – Geochemical and mineralogical criteria for the identification of ash layers in the stratigraphic framework of a foredeep: The early Miocene Mt Cervarola Sandstones, northern Italy. – *Chem. Geol.,* **137**, 23-39.

ARKIN Y, NATHAN Y. & STARINSKY A. (1972). – Paleocene-Eocene environments of deposition in the northern Negev (southern Israel). – *Geol. Survey Israel Bull.*, **56**, 1-18

AZAR D., NEL A., SOLIGNAC M., PAICHELER J.C. & BOUCHET F. (1999). – New genera and species of psychodoid flies from the Lower Cretaceous amber of Lebanon. – *Paleontology*, **42**, (6), 1101-1136.

BANDEL K., SHINAC R. & WEITSCHAT W. (l997). – First insect inclusions from the amber of Jordan (Mid Cretaceous). – *Mitt. Geol. Paleontol. Inst. Univ. Hamburg*, **80**, 213-223.

BARNES S..J., NALDRETT A.J. & GORTON M.P. (1985). – The origin of the fractionation of platinum group elements in terrestrial magmas. – *Chem. Geol.,* **53,** (3-4), 303-323.

BARRERA E. (l994). – Global environmental changes preceding the Cretaceous-Tertiary boundary: early-Upper Maastrichtian transition. – *Geology*, **22**, 877-880.

BOLLE M.P., PARDO A., ADATTE T., VON SALIS K. & BURNS S. (2000). – Climatic evolution on the southeastern margin of the Tethys (Negev, Israel) from the Paleocene to the early Eocene: focus on the late Paleocene thermal maximum. – *J. Geol. Soc.,* London, **157**, 929-941.

BOLLE M.P. & ADATTE T. (2001). – Palaeocene-early Eocene climatic evolution in the Tethyan realm: clay mineral evidence. – *Clay Minerals*, **36**, 249-261

BRALOWER T., PAUL C.K. & LECKIE R. M. (l998). – The Cretaceous-Tertiary boundary cocktail: Chicxulub impact triggers margin collapse and extensive sediment gravity flows. – *Geology,* **26**, 331-334.

CAMOIN G., BELLION Y., DERCOURT J., GUIRAUD R., LUCAS J., POISSON A., RICOU L.-E. & VRIELYNCK B. (1993). – Late Maastrichtian (69.5-65 Ma). *In :* DERCOURT J., RICOU L.-E. & VRIELYNCK B., Eds, Atlas Tethys paleoenvironmental maps, explanatory Notes. – Gauthier-Villars, Paris, 179-197.

Bull. Soc. géol. Fr., 2005, n° 1

CHAMLEY H. (1989). – Clay-sedimentology. – Springer Verlag, Heidelberg, 623p.

CHAMLEY H. (1997). – Clay mineral sedimentation in the Ocean. *In :* PAQUET H. & CLAUER N., Eds, Soils and sediments. – Springer, Heidelberg, 269-302

CHAMLEY H., DECONINCK J.-F. & MILLOT G. (1990). – Sur l'abondance des minéraux smectitiques dans les sédiments marins communs déposés lors des périodes de haut niveau marin du Jurassique au Paléogène. – *C.R. Acad. Sci.,* Paris**, 311,** (2), 1529-1536.

COURTILLOT V., JAEGER J.-J., YANG Z., FERAUD G. & HOFMANN C. (l996). – The influence of continental flood basalts on mass extinctions: where do we stand? – *Geol. Soc. Amer., Sp. Paper,* **307,** 513-526.

DEBRABANT P., FOURCADE E., CHAMLEY H., ROCCHIA R., ROBIN E., BELLIER J.-P., GARDIN S. & THIEBAULT F. (1999). – Les argiles de la transition Crétacé-Tertiaire au Guatemala, témoins d'un impact d'astéroïde. – *Bull. Soc. géol. Fr.,* **170,** 643-660.

DECONINCK J.-F. (1992). – Sédimentologie des argiles dans le Jurassique-Crétacé d'Europe occidentale et du Maroc. – Mém. HDR, Lille I, 266 p.

DIETRICH H.G. (1976). – Zur Entstehung und Erhaltung von Bernstein-Lagerstaetten; 2, Bernstein-Lagerstaetten im Libanon. – *Neues Jahrbuch für geologie and Paleontologie*, **152** (2), 222-279.

ELLIOT C. W. (1993). – Origin of the Mg smectite at the Cretaceous/Tertiary (K/T) boundary at Stevns Klint, Denmark. – *Clays and Clay Minerals*, **41**, 442-452.

ELLIOT C.W., ARONSON J.L., MILLARD H.T. & GIERLOWSKI-KORDESCH E. (1989). – The origin of clay minerals at the Cretaceous/Tertiary boundary in Denmark. – *Geol Soc. Amer. Bull.*, **101**, 702-710.

ELLWOOD B.B., MACDONALD W.D., WHEELER C. & BENOIST S.L. (2003). – The K-T boundary in Oman: identified using magnetic susceptability field measurements with geochemical confirmation. – *Earth Planet. Sci. Lett.,* **206**, 529-540.

FASTOVSKY D. E. (1996). – The evolution and extinction of the dinosaurs. – Cambridge University Press, 460p.

FLEXER A., ROSENFELD A., LIPSON B.S. & HONIGSTEIN A. (1986). – Relative sea level changes during the Cretaceous in Israel. – *AAPG Bull.,* **70** (11), 1685-1699.

GAUCHER G. (1981). – Les facteurs de la pedogenèse. – G. Lelotte. Dison, Belgium, 730 pp.

GIBBS R.J. (1977). – Clay mineral segregation in the marine environment. – *J. Sed. Petr.*, **47**, 237-243.

HARDENBOL J., THIERRY J., FARLEY M.B., GRACIANSKY P.-C. de & VAIL P.R. (1998). – Mesozoic and Cenozoic sequence chronostratigraphic framework of European basins. *In*: P.C. de GRACIANSKY, J. HARDENBOL, T. JACQUIN, P.R. VAIL, Eds, Mesozoic and Cenozoic sequence stratigraphy of European basins. – *Soc. Sediment. Geol., Sp. Publ.*, **60**, 3-13.

HOFFMANN C., FERAUD G. & COURTILLOT V. (2000). – $^{40}Ar/^{39}Ar$ dating of mineral separates and whole rocks from the Western Ghats lava pile: further constraints on duration and age of Deccan traps. – *Earth Planet. Sci. Lett.,* **180**, 13-27.

JARVIS I., MURPHY A. M. & GALE A. (2001). – Geochemistry of pelagic and hemipelagic carbonates; criteria for identifying systems tracts and sea-level change. – *J. Geol. Soc., London*, **158**, (4), 685-696.

JOHNSON C. & KAUFFMAN E. G. (1996). – Maastrichtian extinction patterns of Caribbean Province rudistids. *In*: G. KELLER & N. MACLEOD, Eds, Cretaceous-Tertiary mass extinctions, biotic and environmental changes. – Norton & Company, New York, 231-273.

KARPOFF A.-M., LAGABRIELLE Y., BOILLOT G. & GIRARDEAU J. (1989). – L´authigenèse océanique de palygorskite, par halmyrolyse de péridotites serpentinisées (marge de Galice): ses implications géodynamiques. – *C. R. Acad. Sci.,* Paris, **308**, 647-654.

KELLER G. (1988). – Extinction, survivorship and evolution of planktic foraminifera across the Cretaceous/Tertiary boundary at El Kef Tunisia. – *Mar. Micropal.*, **13**, 239-263.

KELLER G. (2001). – The end-Cretaceous mass extinction in the marine realm: year 2000 assessment. – *Planet. Space Sci.*, **49**, 817-830.

KELLER G. (2002). – *Guembelitria* dominated planktic foraminiferal assemblages mimic early Danian in central Egypt. – *Mar. Micropal.*, **47**, 71-99.

KELLER G. (2003). – Biotic effects of impacts and volcanism. – *Earth Planet. Sci. Lett.,* **6771**, 1-16

KELLER G. & BENJAMINI C. (1991). – Paleoenvironment of the eastern Tethys in the early Paleocene. – *Palaios*, **6**, 439-464.

KELLER G., LI L. & MACLEOD N. (l995). – The Cretaceous/Tertiary boundary stratotype section at El Kef, Tunisia: How catastrophic was the mass extinction? – *Paleogeogr., Paleoclimatol., Paleoecol.,* **119**, 221-254.

KELLER G., ADATTE T., STINNESBECK W., AFFOLTER M., SCHILLI L. & LOPEZ-OLIVA J.G. (2002). – Multiple spherule layers in the late Maastrichtian of northeastern Mexico. – *Geol. Soc. Amer., Sp. Publ.,* **356**, 145-162.

KELLER G., STINNESBECK W., ADATTE T. & STÜBEN D. (2003a). – Multiple impacts across the Cretaceous–Tertiary boundary. – *Earth-Science Rev.*, **1283**, 1-37.

KELLER G., STINNESBECK W., ADATTE T., HOLLAND B., STÜBEN D., HARTING M., LEON C.D. & CRUZ J.D. (2003b). – Spherule deposits in Cretaceous-Tertiary boundary sediments in Belize and Guatemala – *J. Geol. Soc.*, **160**, 5, 783-795

KELLER G., ADATTE T., STINNESBECK W., REBOLLEDO-VIEYRA, URRUTIA-FUCUGAUCHI J., KRAMAR U. & STUEBEN D. (2004). – Chicxulub crater predates the KT mass extinction. – *PNAS,* **101**, 11, 3721-3992.

KRAMAR U. (1997). – Advances in energy-dispersive X-ray fluorescence. – *J. Geochem. Explor.*, **58**, 73-80.

KRAMAR U., STUEBEN D., BERNER Z., STINNESBECK W., PHILIPP H. & KELLER G. (2001). – Are Ir anomalies sufficient and unique indicators for cosmic events? – *Planet. Space Sci.*, **49**, 831-837

KÜBLER B. (1983). – Dosage quantitatif des minéraux majeurs des roches sédimentaires par diffraction X. – *Cah. Inst. Géol. Neuchâtel*, Série ADX, v. 1, 12 p.

KÜBLER B. (1987). – Cristallinite de l'illite, méthodes normalisées de préparations, méthodes normalisées de mesures. – *Cah. Inst. Géol. Neuchâtel*, Série, ADX, v. 1, 13 p.

KUCERA M. & MALMGREN B. A. (l998). – Terminal Cretaceous warming event in the mid-latitude South Atlantic Ocean: evidence from poleward migration of *Contusotruncana contusa* (planktonic foraminifera) morphotypes. – *Palaeogeogr., Palaeoclimatol., Palaeoecol.*, **138**, 1-15.

KYTE F.T. & WASSON J.T. (1986). – Accretion rate of extraterrestrial matter; iridium deposited 33 to 67 million years ago. – *Science*, **232**, 1225-1229

LE-CALLONNEC L., RENARD M., ROCCHIA R., BOURDILLON C. GALBRUN B., RAZIN P. & ROGER J. (1998). – Approche géochimique (isotopes du carbone et iridium) de la limite Crétacé/ Paléocène dans les montagnes d'Oman; un événement « catastrophique » au sein d'une succession d'événements géologiques au cours du Maastrichtien et du Danien. – *Bull. Soc. géol. Fr.*, **169**, (4), 503-514

LI L. & KELLER G. (1998a). – Abrupt deep-sea warming at the end of the Cretaceous. – *Geology*, **26**, 995-99.

LI L. & KELLER G. (1998b). – Maastrichtian diversification of planktic foraminifera at El Kef and Elles, Tunisia. – *Eclogae Geol. Helv.,* **91**, 75-102.

LI L., KELLER G., ADATTE T. & STINNESBECK W. (2000). – Late Cretaceous sea level changes in Tunisia: a multi-disciplinary approach. – *J. Geol. Soc. London*, **157**, 447-458.

LUGER P. (1988). – Maastrichtian to Paleocene facies evolution and Cretaceous/Tertiary boundary in middle and southern Egypt. – *Rev. Esp. Micropal.*, **Num. Extr.**, 83-90.

MACLEOD N. & KELLER G. (1991). – How complete are Cretaceous/Tertiary boundary sections? A chronostratigraphic estimate based on graphic correlation. – *Geol. Soc. Amer. Bull.*, **103**, 1439-1457.

MAGARITZ M., MOSHKOVITZ S., BENJAMINI C., HANSEN H.J., HAKANSSON E. & RASMUSSEN K.L. (l985). – Carbon isotope, bio- and magnetostratigraphy across the Cretaceous-Tertiary boundary in the Zin Valley, Negev, Israel. – *Newsl. Stratigr.*, **15** (2), 100-113.

MOLINA E. , ARENILLAS I. & ARZ J.A. (1998). – Mass extinction in planktic Foraminifera at the Cretaceous/Tertiary boundary in subtropical and temperate latitudes. – *Bull. Soc. géol. Fr.*, **169**, 351-363.

ODIN G.S. (1998). – Green marine clays. – *Dev. Sediment.*, Elsevier, Amsterdam, **45**, 445 p

OLSSON R.K. (l997). – El Kef blind test III results. – *Mar. Micropal.*, **29**, 80-84.

OLSSON R. K., WRIGHT J. D. & MILLER K. G. (2001). – Paleobiogeography of *Pseudotextularia elegans* during the latest Maastrichtian global warming event. – *J. Foram. Res.*, **31** (3), 275-282.

ORTEGA-HUERTAS M., MARTINEZ-RUIZ F., PALOMO I. & CHAMLEY H. (2002). – Review of the mineralogy of the Cretaceous-Tertiary boundary clay: evidence supporting a major extraterrestrial catastrophic event. – *Clay Minerals*, **37**, 395-411.

PARDO A., ORTIZ N. & KELLER G. (1996). – Latest Maastrichtian and K/T boundary foraminiferal turnover and environmental changes at Agost, Spain. *In :* N. MACLEOD, and G. KELLER, Eds., The Cretaceous-Tertiary boundary mass extinction: biotic and environmental events. – W. W. Norton & Co., New York, p. 155-176.

PFEIFER T., STRIBIRNY B., URBAN H. & BANASZAK A. (1997). – PGE, gold and silver distribution in selected profiles of the polish Kupferschiefer. *In :* H. PAPUNEN, Ed, Mineral deposits. Research and exploration –Where do we meet? – Balkema, Rotterdam, 99-102.

PLETSCH T. (1996). – Palaeogeographic controls on palygorskyte occurrence in mid-Cretaceous sediments of Morocco and adjacents basins. – *Clay Mineral.,* **31**, 403-416.

ROBERT C. & CHAMLEY H. (1990). – Paleoenvironmental significance of clay mineral associations at the Cretaceous-Tertiary passage. – *Palaeogeogr., Palaeoclimatol., Palaeoecol.*, **79,** (3-4), 205-219.

ROBERT C. & CHAMLEY H. (1991). – Development of early Eocene warm climates, as inferred from clay mineral variations in oceanic sediments. – *Global and Planetary Change,* **89,** 315-332.

ROBERT C. & KENNETT J. P. (1992). – Paleocene and Eocene kaolinite distribution in the South Atlantic and Southern Ocean: Antarctic climate and paleoceanographic implications. – *Mar. Geol.*, **103**, 99-110.

ROSENFELD A., FLEXER A., HONIGSTEIN A., ALMOGI-LABIN A. & DVORACHEK M. (l989). – First report on a Cretaceous/Tertiary boundary section at Makhtesh Gadol, southern Israel. – *N. Jb. Geol. Paleont. Mh.,* **8**, 474-488.

SHOVAL S. (2000). – Argillation of submarine volcanic rocks; A source for detrital smectite deposited in the Levant Basin during the Tethys divergence and convergence. – *1st Latin American Clay Conference*, Funchal 2000, 96-113.

SMIT J. (1990). – Meteorite impact, extinctions and the Cretaceous/Tertiary boundary. – *Geol. Mijnb.*, **69**, 187-204.

SMIT J. (l999). – The global stratigraphy of the Cretaceous-Tertiary boundary impact ejecta. – *Ann. Rev. Earth Planet. Sci.*, **27**, 75-113.

SMITH L.H., KAUFMAN A. J., KNOLL A.H. & LINK P.K. (1994). – Chemostratigraphy of predominantly siliciclastic Neoproterozoic successions; a case study of the Pocatello Formation and lower Brigham Group, Idaho, USA. – *Geol. Mag.*, **131**, (3), 01-314

SPEIJER R. P. (l994). – Extinction and recovery patterns in benthic foraminiferal paleocommunities across the Cretaceous/Paleogene and Paleocene/Eocene boundaries. – *Geol. Ultraiect.*, Medelingen van de Faculteit Aardwetenschappen, Universiteit Utrecht, 190 p.

STINNESBECK W., SCHULTE P., LINDENMAIER F., ADATTE T., AFFOLTER M., SCHILLI L., KELLER G., STUEBEN D., BERNER Z., KRAMER U. & LOPEZ-OLIVA J.P. (2001). – Late Maastrichtian age of spherule deposits in northeastern Mexico: Implication for Chicxulub scenario. – *Can. J. Earth Sci.*, **38**, 229-238.

STUEBEN D., KRAMAR U., BERNER Z., ECKHARDT J.D., STINNESBECK W., KELLER G., ADATTE T. & HEIDE K. (2002). – Two anomalies of platinum group elements above the Cretaceous-Tertiary boundary at Beloc, Haiti: geochemical context and consequences for the impact scenario. – *Geol. Soc. Amer. Sp. Pap.*, **356**, 163-188.

THIRY M. & JACQUIN T. (1993). – Clay mineral distribution related to rift activity, sea-level changes and paleoceanography in the Cretaceous of the Atlantic Ocean. – *Clay Mineral.*, **28** (1), 61-84.

TUCKER E.M. & WRIGHT V.P. (1990). – Carbonate sedimentology. – Blackwell Scientific publications, London, 482 p.

WEAVER C.E. (1989). – Clays, muds and shales. – *Dev. Sediment.*, **44**, Elsevier, 819 p.

WEAVER C.E. & BECK K.C. (1977). – Miocene of SE USA, a model for chemical sedimentation in a peri-marine environment. – *Dev. Sediment.*, **22**, 234 p.

WOLFART R. (1967). – Geologie von Syrien und dem Libanon. – Beiträge zur regionalen Geologie der Erde, **6**, 306 p.